AMERICAN MUSEUM NOVITATES

Number 3889, 47 pp. December 15, 2017

Osteology of a New Late Cretaceous Troodontid Specimen from Ukhaa Tolgod, Ömnögovi Aimag, Mongolia

RUI PEI,[1] MARK A. NORELL,[2] DANIEL E. BARTA,[3] G.S. BEVER,[4] MICHAEL PITTMAN,[5] AND XING XU [6]

ABSTRACT

A new troodontid dinosaur, *Almas ukhaa*, from the Late Cretaceous deposits of the Djadokhta Formation at Ukhaa Tolgod, Mongolia, is described here. The holotype specimen (IGM 100/1323) comprises an almost complete and articulated cranium and partial articulated postcranial skeleton. This specimen has a small body size and a short snout as in basal paravians, but it exhibits a number of derived troodontid features that differentiate *Almas ukhaa* from the Early Cretaceous troodontids reported from China and unite this new taxon with other Late Cretaceous troodontids. Relative to other troodontids, *Almas ukhaa* is autapomorphic in the presence of a posteriorly curved pterygoid flange, absence of a lateral groove on the anterior part of the dentary, presence of a distinct spikelike process on the ischium, and elongate chevrons. The eggshell associated with IGM 100/1323 can be assigned to Prismatoolithidae indet. based on the smooth surface, eggshell thickness, and microstructural characteristics, and also preserves attributes similar to *Protoceratopsidovum minimum*. A unique relationship between *Byronosaurus* and the perinate troodontids IGM 100/972 and IGM 100/974 is no longer supported based on the new observations of *Almas ukhaa* and *Gobivenator*.

[1] Department of Earth Sciences, the University of Hong Kong, and Division of Paleontology, American Museum of Natural History, New York.
[2] Macaulay Family Curator, Division of Paleontology, American Museum of Natural History, New York.
[3] Richard Gilder Graduate School and Division of Paleontology, American Museum of Natural History, New York.
[4] Division of Paleontology, American Museum of Natural History, New York, and Center for Functional Anatomy & Evolution, Johns Hopkins University School of Medicine, Baltimore.
[5] Vertebrate Palaeontology Laboratory, Department of Earth Sciences, the University of Hong Kong.
[6] Institute of Vertebrate Paleontology and Paleoanthropology, the Chinese Academy of Sciences, Beijing.

 ISSN 0003-0082

INTRODUCTION

Late Cretaceous deposits in the Gobi Desert have yielded many important and exquisitely preserved fossils that have significantly improved our understanding of the systematics and paleobiology of nonavian dinosaurs as well as the accrual of those features that distinguish modern birds within the extant vertebrate fauna (Osborn, 1924; Maleev, 1954; Barsbold, 1974; Norell et al., 1995; Chiappe et al., 1998; Clarke et al., 2001; Brusatte et al., 2009; Tsuihiji et al., 2014; and others). Of the many fossil beds across Mongolia and northern China, the Campanian beds of the Djadokhta Formation are famous for both the abundance and exquisite preservation of various maniraptorans (Osborn et al., 1924; Jerzykiewicz and Russell, 1991; Norell et al., 1995; Norell and Makovicky, 1997; Clark et al., 2001; Norell and Clarke, 2001; Chiappe et al., 2001; Turner et al., 2007a; Dingus et al., 2008; Balanoff and Norell, 2012; Tsuihiji et al., 2014). Here we report a small-bodied troodontid specimen from the Djadokhta Formation (late Campanian) sediments of Ukhaa Tolgod, Mongolia (Dingus et al., 2008). This skeleton, IGM (Institute of Geology, Mongolia) 100/1323 (fig. 1), was collected by the joint expedition of American Museum of Natural History and Mongolian Academy of Sciences in 1993.

At least five troodontid taxa have been reported and named in the Djadokhta Formation and Djadokhta Formation–equivalent fossil beds of the Gobi Desert: *Saurornithoides mongoliensis* from Bayan Dzak, Mongolia, *Byronosaurus jaffei* from Ukhaa Tolgod, Mongolia, *Linhevenator tani* and *Philovenator curriei* from the Wulansuhai Formation of Inner Mongolia, China, and *Gobivenator mongoliensis* from Zamin Khond, Mongolia (Osborn, 1924; Norell et al., 2000; Xu et al., 2011a, 2012; Tsuihiji et al., 2014). Two perinate troodontid specimens were reported from Ukhaa Tolgod in 2009, and were regarded as the perinate individuals of *Byronosaurus* (Bever and Norell, 2009). Additionally, another large taxon may be present in the Ukhaa Tolgod beds (Norell and Hwang, 2004). To clarify, the fossil beds at Ukhaa Tolgod, Zamin Khond, and Wulansuhai Formation are very similar or even equivalent to the Djadokhta Formation, but cannot be referred to the Djadokhta Formation sensu stricto, as much of their fauna is different from that at the known Djadokhta Formation sites (see Dingus et al., 2008; Makovicky, 2008), despite the similarities (see Gao and Norell, 2000, and discussion in Xu et al., 2015). In this study, all Djadokhta Formation–equivalent beds are referred to as Djadokhta Formation.

All named troodontid taxa from the Djadokhta Formation have adult skull lengths of 16–22 cm. The *Philovenator curriei* holotype skeleton lacks a skull, but if limb lengths are compared to IGM 100/1323, its skull would be about the same size. IGM 100/1323 has a skull length of about 8 cm, significantly smaller than other adult Djadokhta troodontids except *P. curriei*. As the first small-sized troodontid taxon represented by good material reported from the Late Cretaceous, IGM 100/1323 has both primitive and derived troodontid features, and therefore provides critical information on the evolution of Troodontidae and Paraves. IGM 100/1323 has been included in previous studies of coelurosaurian phylogeny (Turner et al., 2011, 2012; Brusatte et al., 2014), but was not officially described in detail. A new analysis of the phylogenetic position of this taxon is part of a larger project currently in production. Here we provide a detailed description of this specimen and its implications related to the ontogeny of troodontid dinosaurs and their diversity in the Djadokhta Formation.

SYSTEMATIC PALEONTOLOGY

THEROPODA MARSH, 1881

COELUROSAURIA HUENE, 1920

MANIRAPTORA GAUTHIER, 1986

TROODONTIDAE GILMORE, 1924

***Almas ukhaa*,** new taxon

Holotype: IGM 100/1323, a skull and mandible and with partial articulated postcranial skeleton (figs. 1, 2, 3, 6, 7, 8, 9).

Type Locality: Ukhaa Tolgod, Ömnögovi Aimag, Mongolia.

Formation: Djadokhta Formation, Campanian (Dingus et al., 2008), 75–71 Ma (Dashzeveg et al., 2005)

Etymology: *Almas* is in reference to the wild man or snowman of Mongolian mythology (Rincen, 1964). *Ukhaa* refers to the locality of Ukhaa Tolgod, discovered in 1993, where the specimen was collected.

Diagnosis: *Almas ukhaa* can be referred to troodontids based on the following suite of characters: lacrimal with a prominent supraorbital crest (fig. 3), lacrimal with an anterior process significantly longer than posterior process (fig. 3), numerous dentary and maxillary teeth that are closely packed anteriorly (figs. 2, 3, 4), laterally recessed squamosal (fig. 6), and fully arctometatarsalian pes (fig. 15).

Almas ukhaa can be distinguished from all other troodontids by the combination of these derived characters: posteriorly curved pterygoid flange (fig. 5), absence of a lateral groove on the anterior part of the dentary (fig. 2), distinct spikelike process extending from the anterior edge of the obturator process at the distal one-third of the ischium (fig. 13), the third chevron more than three times as long as the corresponding caudal vertebra (fig. 10).

Material

IGM (Institute of Geology, Mongolia) 100/1323 is composed of a nearly complete skull and partial postcranium (figs. 2, 3). The cranial elements of the holotype are semiarticulated, with several bones displaced from their original positions due to lateral compression. The parietal, the left squamosal, and the prootic were found adjacent to the articulated skull (figs. 6, 7, 8). The postcranial skeleton (fig. 9) is partially preserved with several sacral and proximal caudal vertebrae, a partial pelvic girdle, and partial hind limbs (missing pedal digits). Six small eggshell fragments are scattered around the skeleton.

Limb-bone thin sections failed to reveal the absolute age of the holotype or whether it was somatically mature; the fact that the bones were fungally altered after deposition probably has caused this lack of clarity. Because growth stage could not be determined quantitatively, morphology was used to estimate the ontogenetic stage of the holotype. IGM 100/1323 displays several features of immaturity, such as an unfused braincase, unfused sacral vertebrae, and a

FIGURE 1. Type specimen of *Almas ukhaa*, IGM 100/1323.

rugose surface of limb bones. However, the general ossification of the skeleton, fusion of the parietals and the fusion of proximal tarsals may suggest IGM 100/1323 is close in size to a somatic adult. Although *Almas ukhaa* displays some juvenile features such as an enlarged orbit and a short snout, these features are likely paedomorphic and are common in basal and small paravians, such as *Sinovenator*, *Mei*, *Archaeopteryx*, *Anchiornis*, and *Microraptor* (Xu et al., 2002; Xu and Norell, 2004; Hu et al., 2009; Bhullar et al., 2012; Pei et al., 2014).

MORPHOLOGICAL DESCRIPTION

Skull and Mandible

The skull of *Almas ukhaa* is subtriangular in lateral view (figs. 2, 3). The skull has a primitive paravian profile resembling *Archaeopteryx*, *Anchiornis*, *Microraptor*, *Sinovenator*, *Mei* and *Jianianhualong* (Xu et al., 2002; Xu and Norell, 2004; Hu et al., 2009; Pei et al., 2014; 2017; Xu et al., 2017). The skull is deep and the length of the skull is about 2.5 times the height. The preorbital region makes up 61% of the total skull length, differing from *Sinornithoides* and more derived troodontids where the rostrum is much longer (Russell and Dong, 1993; Makovicky et al., 2003; Norell et al., 2009; Tsuihiji et al., 2014).

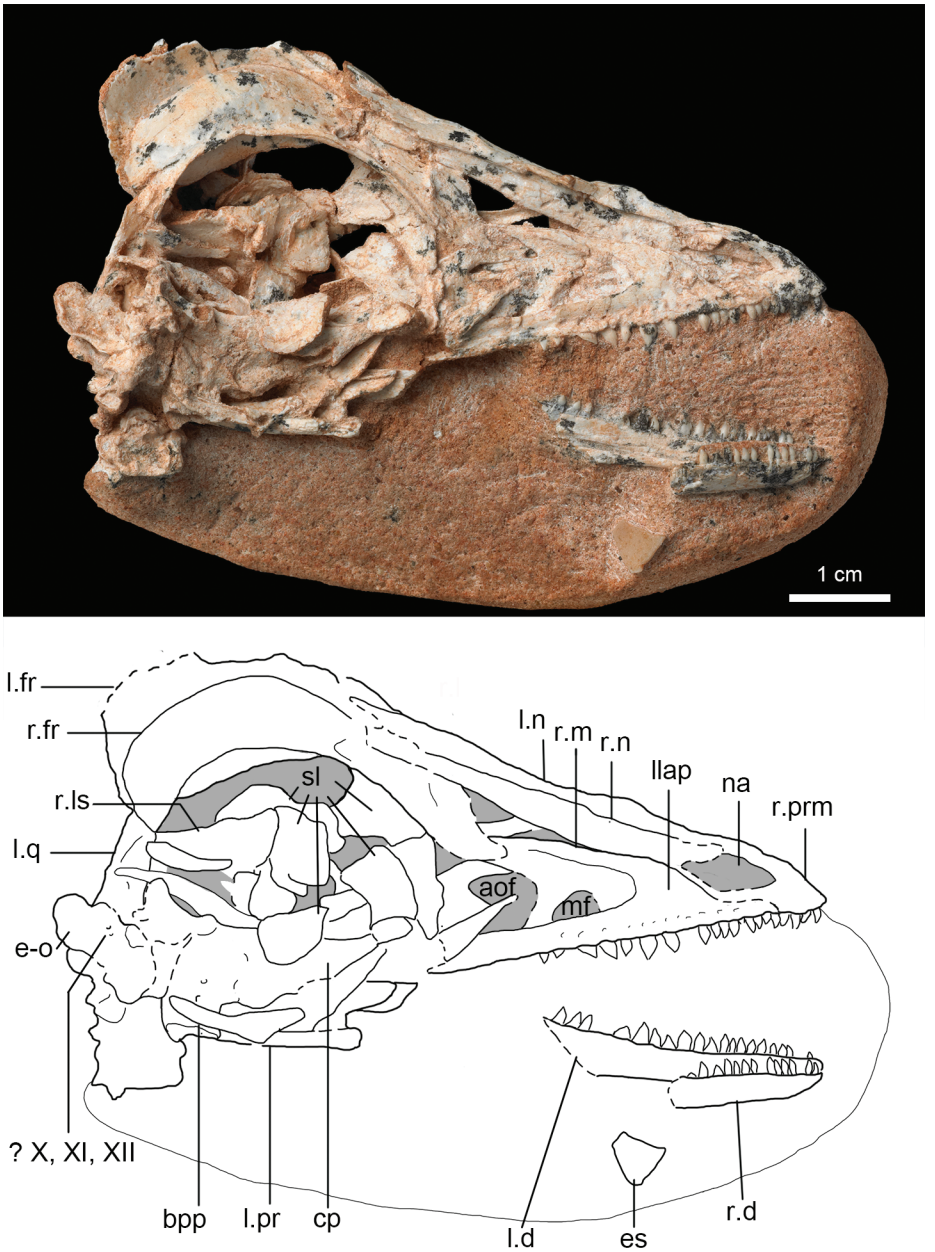

FIGURE 2. Skull of IGM 100/1323 in right lateral view.

Premaxilla: Both premaxillae are preserved in the holotype (figs. 2, 3, 4). The anterior tip of the rostrum is pointed in dorsal view, as in *Archaeopteryx*, *Anchiornis*, and *Mei*, but is different from derived troodontids such as *Byronosaurus* and *Saurornithoides*, in which the rostrum is rounded anteriorly in dorsal view (Makovicky et al., 2003; Xu and Norell, 2004; Mayr et al., 2005; Norell et al., 2009; Hu et al., 2009). The anterior margin of the premaxilla posterodorsally inclines in lateral view, similar to *Mei*, *Anchiornis*, and *Archaeopteryx* (Xu and

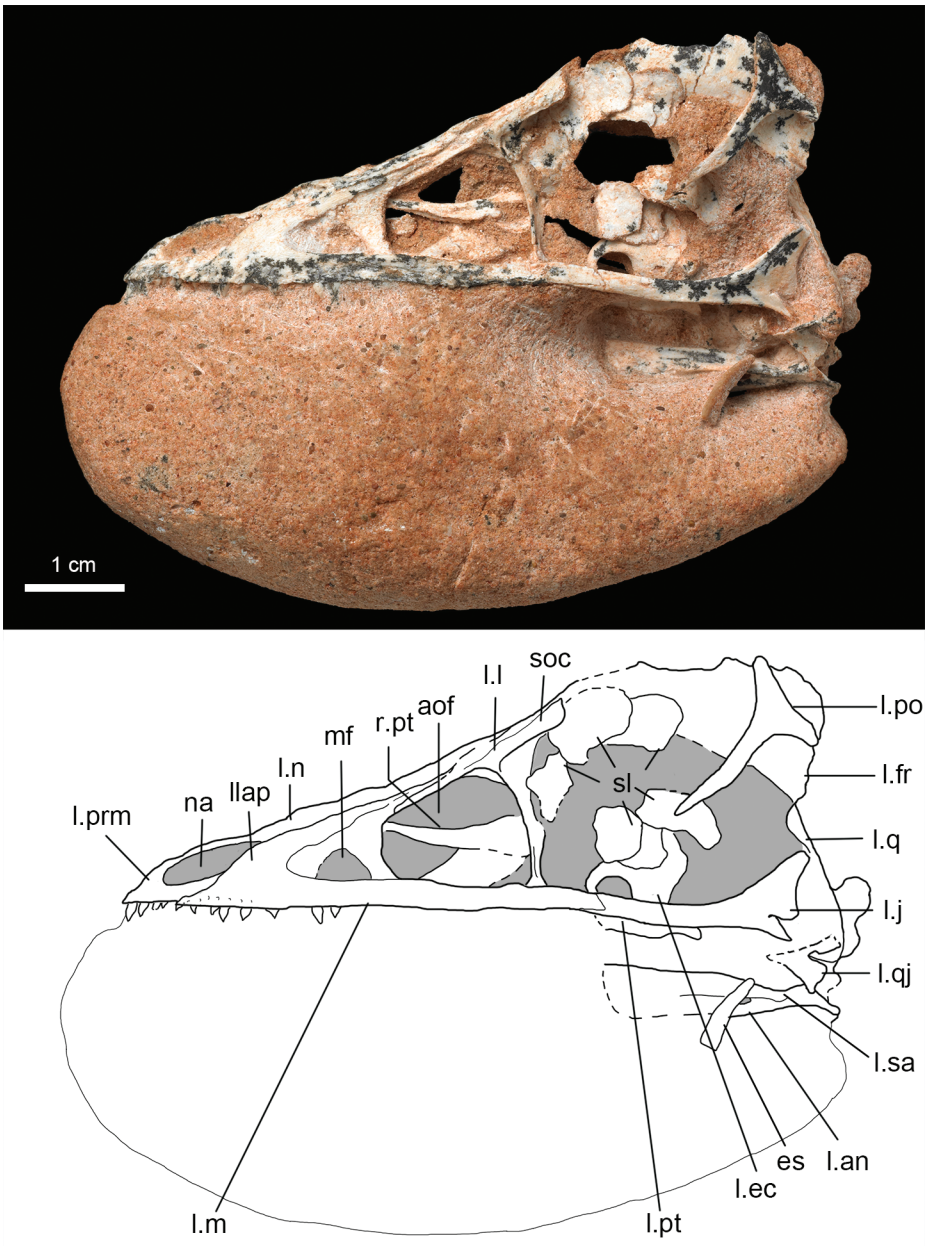

FIGURE 3. Skull of IGM 100/1323 in left lateral view.

Norell, 2004; Pei et al., 2017). The premaxilla of *Almas ukhaa* is shallow ventral to the external naris, which is like other troodontids and some basal paravians (Xu et al., 2002; Makovicky et al., 2003; Mayr et al., 2005, Norell et al., 2009; Pei et al., 2014). In contrast, the premaxilla ventral to the external naris is dorsoventrally deep in derived dromaeosaurids, such as *Velociraptor*, *Dromaeosaurus*, and *Tsaagan* (Barsbold and Osmólska, 1999; Currie, 1995; Norell et al., 2006). The nasal process of the premaxilla is slender, about twice as long as the premaxillary

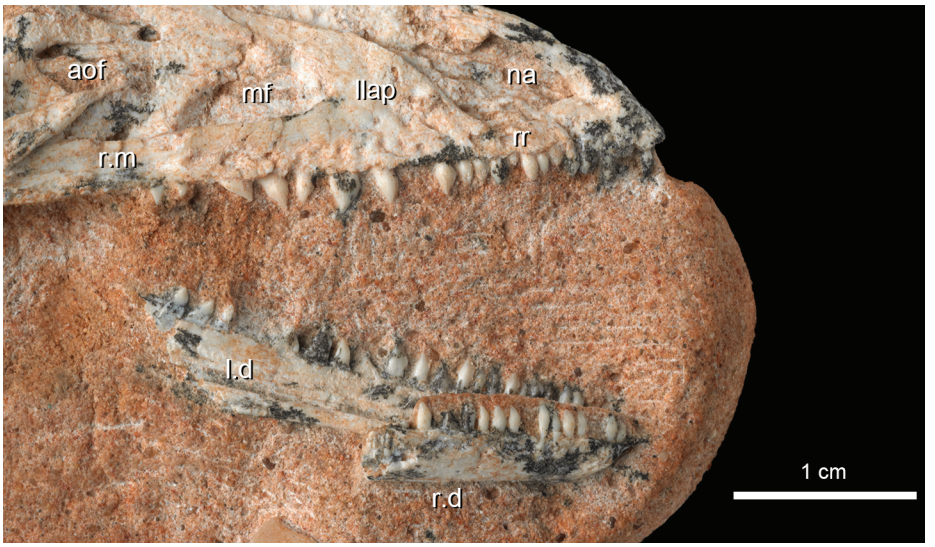

FIGURE 4. Dentition and rostrum of IGM 100/1323.

body, forming the anterior and anterodorsal border of the external naris. As in other deinonychosaurians, the anterior/lower portion of the nasal process of the premaxilla extends posterodorsally, and the posterior/upper portion of the nasal process becomes relatively horizontal (figs. 2, 3). This is different from the condition in *Anchiornis* and *Archaeopteryx* in which the nasal process is straight (Pei et al., 2017). As in all described troodontids and some basal paravians, the internarial bar is dorsoventrally flattened as can be observed on the right premaxilla (Makovicky et al., 2003; Norell et al., 2009; Lü et al., 2010; Pei et al., 2017).

The subnarial process of the premaxilla is reduced and partially obfuscated by the anterior ramus of the maxilla in lateral view as a primitive paravian condition (Xu et al., 2002; Makovicky et al., 2003). The subnarial process contacts the nasal and forms the floor of the external naris. In contrast, the elongate subnarial process of derived dromaeosaurids projects above the maxilla anteriorly and contacts the nasal in lateral view (Currie, 1995; Norell and Makovicky, 2004). The external naris is anteroposteriorly elongate, with the long axis more than twice that of the short dorsoventral axis. In this case, it is similar to *Sinovenator*, *Byronosaurus*, and some basal avialans, such as *Anchiornis* (Xu et al., 2002; Makovicky et al., 2003; Hu et al., 2009; Pei et al., 2017). In derived troodontids such as *Saurornithoides* and *Zanabazar*, the external naris is anteroposteriorly shortened, regardless of the elongation of the rostrum (Barsbold, 1974; Norell et al., 2009). The size-comparable avialan *Anchiornis* and the dromaeosaurid *Microraptor* also have an elongated external naris (Pei et al., 2014, 2017), but larger and derived dromaeosaurid taxa such as *Velociraptor* and *Tsaagan* have shorter external nares (Barsbold and Osmólska, 1999; Norell et al., 2006). The anterior margin of the external naris is located above the third premaxillary tooth in *Almas ukhaa*, which is common in nonavialan paravians (Pei et al., 2017).

Four premaxillary teeth are present on each side (fig. 4). The tooth crowns are lancet shaped and slightly recurved. The premaxillary teeth are perpendicular to the ventral edge of

the premaxilla. The premaxillary teeth are similar in size, as in other troodontids and toothed avialans. In contrast, the first two premaxillary teeth are significantly larger than the third and fourth teeth in dromaeosaurid dinosaurs (Xu, 2002; Norell and Makovicky, 2004). The premaxillary teeth of *Almas ukhaa* are similar in size to the anteriormost maxillary teeth, which is a feature shared with other non-dromaeosaurid paravians.

Maxilla: Both maxillae are completely preserved in the holotype (figs. 2, 3). The anterior ramus of the maxilla is slender, and attaches to the labial side of the premaxilla (fig. 4). A distinct anterior ramus is observed in troodontids, basal avialans and some basal dromaeosaurids, such as *Shanag* (Turner et al., 2007a). As in the derived troodontids *Byronosaurus*, *Saurornithoides*, and *Zanabazar* (Makovicky et al., 2003; Norell et al., 2009), the anterior ramus is dorsoventrally shallower than the ventral ramus of the maxilla. This is different from the Early Cretaceous troodontids *Jinfengopteryx*, *Sinovenator*, *Mei*, and *Sinornithoides*, in which the anterior ramus is as deep as the ventral ramus of the maxilla (Russell and Dong, 1993; Xu et al., 2002; Xu and Norell, 2004; Ji and Ji, 2007).

The lateral lamina of the ascending process of the maxilla is broad in the holotype (figs. 2–4). It is as dorsoventrally high as the maxillary fenestra, which is common in derived troodontids like *Byronosaurus*, *Gobivenator*, *Saurornithoides*, and *Zanabazar* (Makovicky et al., 2003; Norell et al., 2009; Tsuihiji et al., 2014). In contrast, the lateral lamina of the ascending process is reduced and less than half the height of the maxillary fenestra in *Jinfengopteryx*, *Sinovenator*, *Mei*, and *Sinornithoides*, which probably represents a primitive condition (Russell and Dong, 1993; Xu et al., 2002; Xu and Norell, 2004; Ji et al., 2005). The dorsal ramus of the ascending process is confluent with the lateral lamina. The dorsal ramus of the maxilla forms the anterodorsal margin of the antorbital fossa and sutures to the nasal dorsally. The preantorbital-fossa component of the maxilla (the anterior ramus and the lateral lamina of the ascending process) of *Almas ukhaa* is 18% of the total length of the maxilla. This is comparable to most paravians, such as *Anchiornis* (25%), *Microraptor* (21%), and *Sinovenator* (~20%), but significantly shorter than in *Archaeopteryx* (45%) and more derived avialans.

The ventral ramus of the maxilla is posterior to the lateral lamina of the ascending process and ventral to the antorbital fossa. It bears a row of foramina on the lateral surface. The lateral surface of the ventral ramus is grooved, as in *Byronosaurus*, *Gobivenator*, and IGM 100/972 (Makovicky et al., 2003; Bever and Norell, 2009; Tsuihiji et al., 2014). The dorsal and ventral edges of the ventral ramus are almost parallel, as is typical of troodontids but different from the posteriorly tapering condition observed in basal avialans and dromaeosaurids (e.g., *Microraptor*, *Velociraptor*, *Achillobator*, *Anchiornis*, and *Archaeopteryx*). The dorsal edge of the ventral ramus defines the ventral margin of a large antorbital fossa. Posteriorly, the ventral ramus abuts the anterior end of the suborbital process of the jugal.

The anterior margin of the antorbital fossa is located posterior to the posterior margin of the external naris (figs. 2, 3), as in the derived troodontids *Byronosaurus*, *Saurornithoides*, and *Zanabazar* (Makovicky et al., 2003; Norell et al., 2009), but different from basal troodontid taxa like *Jinfengopteryx*, *Sinovenator*, and *Mei* (Xu et al., 2002; Xu and Norell, 2004; Ji et al., 2005) in which the posterior margin of the naris is above the antorbital fossa. A well-defined pro-

maxillary fenestra is not visible laterally at the anterior end of the antorbital fossa, unlike *Jinfengopteryx*, *Mei*, *Sinovenator*, *Sinornithoides*, and *Geminiraptor* (Russell and Dong, 1993; Xu et al., 2002; Xu and Norell, 2004; Ji et al., 2005; Senter et al., 2010), but is the same as the condition in derived troodontids *Byronosaurus*, *Xixiasaurus*, *Saurornithoides*, and *Zanabazar* (Makovicky et al., 2003; Norell et al., 2009; Lü et al., 2010).

The maxillary fenestra is located posterior to the anterior margin of the antorbital fossa (figs. 2, 3, 4). It is slightly anteroposteriorly elongate as in IGM 100/972 and IGM 100/974 (Bever and Norell, 2009), which is an intermediate condition between the relatively round maxillary fenestra seen in *Sinovenator* and *Anchiornis* (Xu et al., 2002; Pei et al., 2017), and the significantly elongate maxillary fenestra of derived troodontids, such as *Byronosaurus* and *Zanabazar* (Makovicky et al., 2003; Norell et al., 2009). The maxillary fenestra is much smaller than the antorbital fenestra, around 10% of the area of the antorbital fenestra, as also found in derived troodontids (Makovicky et al., 2003; Norell et al., 2009). In more basal troodontids such as *Sinovenator* and *Jinfengopteryx*, the maxillary fenestra is proportionally larger, usually more than 25% the area of the antorbital fenestra (Xu et al., 2002; Ji et al., 2005). Although derived dromaeosaurids also have proportionally smaller maxillary fenestrae, they are much smaller and more dorsally positioned compared to derived troodontids (Norell and Makovicky, 2004; Turner et al., 2012). The antorbital fenestra of *Almas ukhaa* is quadrangular, with an anterior margin that is shorter than the posterior margin, as in *Byronosaurus* and *Gobivenator*. However, it is not as elongate as in these two taxa (Makovicky et al., 2003, Tsuihiji et al., 2014).

The maxillary fenestra and the antorbital fenestra are separated by an interfenestral bar that inclines anterodorsally. The interfenestral bar is inset from the lateral surface of the maxilla, as in *Sinovenator*, *Xixiasaurus*, *Saurornithoides*, and *Gobivenator* (Xu et al., 2002; Norell et al., 2009; Lü et al., 2010; Tsuihiji et al., 2014), but differs from that of *Byronosaurus* (Makovicky et al., 2003) in which it is confluent with the side wall of the maxilla. An interfenestral canal connects the maxillary and antorbital fenestrae medial to the interfenestral bar as in IGM 100/972, *Byronosaurus* and *Zanabazar* (Makovicky et al., 2003; Bever and Norell, 2009, Norell et al., 2009).

Sixteen maxillary teeth are observed on the right maxilla in the holotype (fig. 4), and 17 maxillary tooth positions are estimated considering the toothrow length. The number of maxillary teeth is similar to that of many troodontids, such as *Sinovenator*, *Zanabazar*, *Saurornithoides*, and IGM 100/972 (Xu et al., 2002; Norell et al., 2009; Bever and Norell, 2009), but it is significantly fewer than the number of teeth in *Byronosaurus* (Makovicky et al., 2003: >30 maxillary teeth on each side). The maxillary teeth are closely packed anteriorly as in most troodontids. The anteriormost maxillary teeth are slightly smaller, but the middle and posterior ones are larger, which is typical of most other deinonychosaurians (Norell and Makovicky, 2004; Makovicky and Norell, 2004). The middle and posterior maxillary teeth incline posteroventrally. The maxillary teeth are constricted between the crowns and the root, which is primitive for paravians. No serrations are developed on the tooth crown of *Almas ukhaa*. This feature is common in other troodontids such as *Mei*, *Jinfengopteryx*, *Gobivenator*, and *Byronosaurus* (Makovicky et al., 2003; Xu and Norell, 2004; Ji and Ji, 2007; Tsuihiji et al., 2014), but unlike

the majority of troodontids (Makovicky and Norell, 2004) and even small dromaeosaurids like *Shanag* (Turner et al., 2007a). The maxillary toothrow extends only the anterior 75% of the maxillary ventral ramus, which is a derived troodontid condition found in the unnamed troodontid IGM 100/1126, *Byronosaurus*, *Gobivenator*, *Saurornithoides*, and *Zanabazar* (Makovicky et al., 2003; Norell et al., 2009; Tsuihiji et al., 2014). In the basal troodontids *Mei* and *Sinovenator*, the maxillary toothrow can extend along over 90% of the ventral ramus of the maxilla (Xu et al., 2002; Xu and Norell, 2004).

Nasal: The nasals of *Almas ukhaa* are paired and well preserved (figs. 2, 3). The nasal is elongate, as is typical of maniraptorans, with a width about 14% of the length. Anteriorly, the nasal forms the posterolateral boundary of the large external naris. A series of foramina are developed dorsally along the anterolateral margin of the nasal, which is also observed in *Byronosaurus* and *Saurornithoides* (Makovicky et al., 2003; Norell et al., 2009). The nasal posteriorly tapers, forming a pointed posterior end that is medial to the supraorbital crest of the lacrimal. A posteriorly positioned cleft between the lacrimal and the nasal displays a W-shaped suture among the nasal, the lacrimal, and the frontal, which is common in paravians. The nasals overlap the frontals dorsally and the lacrimals attach posterolaterally to the nasals. The suture area (the region occupied by the W-shaped suture) is anteroposteriorly short in basal paravians such as *Anchiornis* and *Archaeopteryx* (Mayr et al., 2005; Pei et al., 2017). However, this region is anteroposteriorly elongate in the derived troodontid *Zanabazar* and *Almas ukhaa*, as well as some dromaeosaurids, such as *Velociraptor* (Osborn, 1924; Norell et al., 2009). The elongation of this region is observed in both long-snouted (e.g., *Zanabazar* and *Velociraptor*) and short-snouted (*Almas*) individuals, and is not necessarily associated with the elongation of the snout in these taxa.

Frontal: The frontals of the holotype are paired, and they are dislocated from life position (figs. 2, 3). The frontal is strongly vaulted above the orbit, and is about as long as the nasal as in basal paravians such as *Sinovenator, Anchiornis, Archaeopteryx*, and *Microraptor*. The frontal of *Almas ukhaa* has a similar shape and proportion to *Troodon*, *Zanabazar*, and *Gobivenator* (Norell et al., 2009; Tsuihiji et al., 2014), but unlike the elongate frontal of *Mei* (Xu and Norell, 2004). The anterior end of the frontal is covered by the nasal and the lacrimal if the preserved state is in life position, and thus would have inserted between the nasals as in *Zanabazar* and *Troodon*, as indicated by the shape of the posterior end of the overlaying nasal (Currie, 1985; Norell et al., 2009). Anterolaterally, the frontal has a smooth lateral edge, and lacks a notch to receive the lacrimal that is present in dromaeosaurids (Norell and Makovicky, 2004). A shallow longitudinal groove is developed lateral to the suture of the frontals, and thus a low ridge likely formed along the midline of the frontals as in *Zanabazar* and *Gobivenator* (Norell et al., 2009; Tsuihiji et al., 2014).

The frontal forms the dorsal margin of the round orbit. A supraorbital rim is developed along the orbital margin as in a wide range of paravians, such as *Anchiornis*, *Zanabazar*, and *Microraptor* (Hu et al., 2009; Norell et al., 2009; Pei et al., 2014). The supraorbital rim is confluent posteriorly with the ventral edge of the postorbital. Posteriorly, a faint ridge is present at the anterolateral corner of the anterior margin of the upper temporal fenestra. A depression is located posteroventral to this ridge and medial to the postorbital as the anterior

wall of the upper temporal fenestra, which is a condition that is also observed in *Gobivenator*, *Zanabazar*, and dromaeosaurids (Norell et al., 2009; Tsuihiji et al., 2014). Ventrally, the crista calvarii frontalis is almost perpendicular to the skull roof, which defines a distinct groove between the crista calvarii frontalis and the supraorbital rim. This surface is smooth in *Archaeopteryx* and *Zanabazar*, but a similar, less distinct groove is also observed in the dromaeosaurid *Microraptor* (Norell et al., 2009; Pei et al., 2014). No vascular imprint is observed on the ventral surface of the frontal.

Lacrimal: The left lacrimal is preserved in the holotype, but the right lacrimal is shattered. The left lacrimal is trifurcate and T-shaped in lateral view as typical of paravian dinosaurs (fig. 3).

The anterior process of the lacrimal is long and slender and forms the entire dorsal margin of the antorbital fenestrae (fig. 3). The anterior process is longer than the posterior process as is typical of non-Jehol troodontids (e.g., Makovicky et al., 2003; Norell et al., 2009). The anterior process of the lacrimal of *Almas ukhaa* is less than two times the length of the posterior process, in contrast to *Byronosaurus*, *Gobivenator*, *Saurornithoides*, *Zanabazar*, and *Troodon*, in which the anterior process of the lacrimal is significantly elongate (Makovicky et al., 2003; Norell et al., 2009; Tsuihiji et al., 2014). This difference is probably related to the shortened rostrum of *Almas ukhaa*. In avialans, dromaeosaurids, and basal troodontids, the anterior process of the lacrimal is as long as the posterior process (Ji et al., 2005; Norell et al., 2006; Hu et al., 2009). The anterior end of the anterior process is laterally overlapped by the dorsal ramus of the maxilla in *Almas ukhaa*. As in *Byronosaurus*, IGM 100/972, *Saurornithoides*, and *Microraptor* (Makovicky et al., 2003; Makovicky and Norell, 2004; Norell et al., 2009; Pei et al., 2014), a large pneumatic fossa lies at the posterodorsal corner of the antorbital fenestra in *Almas ukhaa*, between the anterior and ventral processes of the lacrimal. This pneumatic fossa is absent in the other Djadokhta troodontid, *Gobivenator* (Tsuihiji et al., 2014).

The posterior process of the lacrimal is slightly shorter, but is more robust than the anterior process (fig. 3). It is mediolaterally expanded and rectangular in dorsal view. The posterior process forms a robust supraorbital crest as is typical of troodontids (Turner et al., 2012). The posterior edge of the supraorbital crest forms a distinct angle with the lateral margin of the frontal. It is similar to the condition in troodontids such as *Sinovenator*, *Mei*, and *Gobivenator* (Xu et al., 2002; Xu and Norell, 2004; Tsuihiji et al., 2014). In dromaeosaurid dinosaurs the lateral edge of the posterior process of the lacrimal is laterally confluent with the supraorbital rim of the frontal (Norell et al., 2006). A pneumatic fossa is present laterally on the lacrimal of the holotype where the ventral and posterior processes meet (fig. 3). A similar fossa is also observed in most deinonychosaurians, but it is located more posteriorly on the ventral process and at the anterodorsal corner of the orbit, as in *Zanabazar*, *Gobivenator*, and *Byronosaurus* (Makovicky et al., 2003; Norell et al., 2009; Tsuihiji et al., 2014).

The ventral process of the lacrimal is anteroposteriorly flattened as in many maniraptorans (Makovicky et al., 2003; Norell et al., 2006; Balanoff and Norell, 2012). The ventral end of this process contacts the suborbital process of the jugal on the medial side. Unlike *Byronosaurus*, *Gobivenator*, and *Saurornithoides*, the ventral process of *Almas ukhaa* is perpendicular to the toothrow, and does not curve anteriorly.

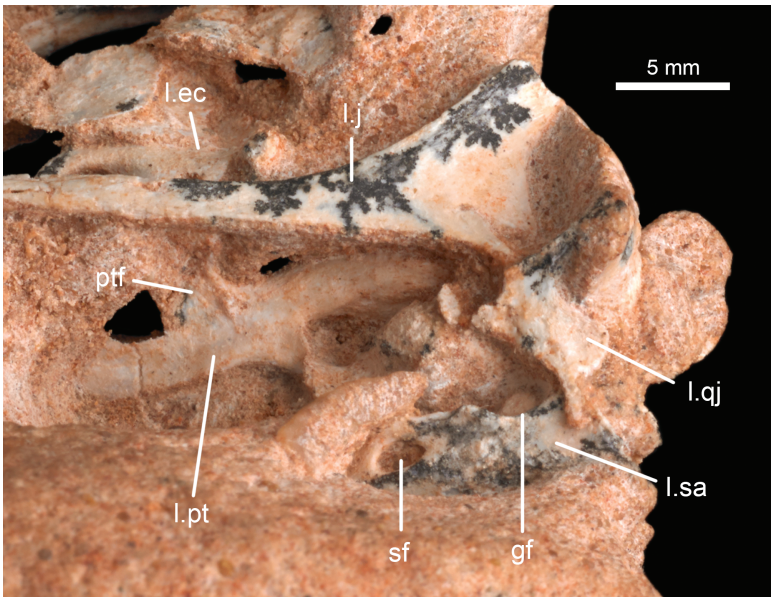

FIGURE 5. Partial left skull of IGM 100/1323 in lateroventral view.

Jugal: The left jugal is well exposed, but the right jugal is missing (figs. 3, 5). The jugal is L-shaped in lateral view. It is lightly built and slender as in other troodontids and avialans (Mayr et al., 2005; Gao et al., 2012; Tsuihiji et al., 2014), but different from the broad and plate-like jugal of derived dromaeosaurids (e.g., Norell et al., 2006). The suborbital process of the jugal is horizontally positioned. It is straplike and much longer than the postorbital process. The suborbital process is as dorsoventrally shallow as the ventral ramus of the maxilla, as in *Gobivenator* and *Saurornithoides* (Norell et al., 2009; Tsuihiji et al., 2014). The anterior end of the suborbital process is forked, as in *Jinfengopteryx* and *Gobivenator*, and it is overlapped by the ventral ramus of the maxilla laterally, contributing to the posteroventral corner of the antorbital fenestra. A horizontal groove is developed along the posterior portion of the suborbital process laterally, which is also present in *Sinovenator*, *Microraptor*, and *Anchiornis* (Pei et al., 2014; Pei et al., 2017). The jugal is posteriorly forked (figs. 3, 5), with a notch developed on the posteroventral corner as in a wide range of paravians (e.g., *Archaeopteryx*, *Anchiornis*, *Velociraptor, Linheraptor*, *Linhevenator*, *Gobivenator*, *Mei*). The postorbital process of the jugal forms a continuous arc with the suborbital process. A short and shallow groove runs posterior to the orbital margin on the postorbital process as in *Tsaagan* and *Gobivenator* (Norell et al., 2006; Tsuihiji et al., 2014).

Postorbital: The left postorbital of the holotype is well preserved and exposed in lateral view (fig. 3). Only the anterior process of the right postorbital is preserved in this specimen. The postorbital is trifurcate, and it contributes to the postorbital bar and the dorsal temporal arcade. The ventral process of the postorbital is slender and ventrally tapers, longer than the postorbital process of the jugal. The ventral process is anteroposteriorly narrow, unlike the broad ventral process of *Zanabazar* and *Gobivenator* (Norell et al., 2009; Tsuihiji et al., 2014).

The ventral process of the postorbital has a smooth anterior margin and lacks the tubercle present in *Zanabazar* (Norell et al., 2009).

The anterior process of the postorbital is about half the length of the ventral process. The anterior process attaches to and is confluent with the frontal, forming the posterodorsal margin of the orbit. The anterior process slightly curves upward at the anterior tip (fig. 3). The posterior process of the postorbital is shorter than the anterior process, and the posterior end is ventrally curved as in *Zanabazar* (Norell et al., 2009).

Quadratojugal: A fragmentary element posteroventral to the left jugal likely represents the quadratojugal of the holotype (figs. 3, 5). However, the orientation of the quadratojugal cannot be determined due to the heavy distortion of the posterior elements of the skull. The quadratojugal is mediolaterally flat. It is generally L-shaped, matching the profile of quadratojugal in other troodontids and basal avialans (Mayr et al., 2005; Tsuihiji et al., 2014; Pei et al., 2017). As in *Mei* and *Gobivenator* (Xu and Norell, 2004; Tsuihiji et al., 2014), the quadratojugal is reduced, and thus is not likely to reach the squamosal.

Quadrate: The left quadrate of the holotype is dislocated and partially exposed in lateral view (figs. 2, 3). The quadrate blade is subtriangular in lateral view. The quadrate head is mediolaterally expanded. A longitudinal groove is developed anteriorly on the lateral surface of the jugal wing. The upper portion of the quadrate blade has a smooth anterior edge, whereas a notch is developed on the anterior edge of the lower portion, as in *Mei* (Xu and Norell, 2004). The quadrate foot is robust and mediolaterally expanded, and bicondylar, as is common of paravians (Norell and Hwang, 2004; Mayr et al., 2005; Hu et al., 2009; Pei et al., 2014). The lower portion of the quadrate shaft bearing the condyles is vertically oriented, in agreement with other paravians, such as *Mei* and *Microraptor* (Xu and Norell, 2004; Gao et al., 2012; Pei et al., 2014). A deep depression is developed on the posterior surface of the quadrate in *Almas ukhaa*, as in *Sinovenator* and *Mei* (Xu et al., 2002; Xu and Norell, 2004). The posterior edge of the quadrate probably inclines posterodorsally in lateral view, as in other troodontids and avialans (Tsuihiji et al., 2014; Pei et al., 2017).

Squamosal: The left squamosal of IGM 100/1323 is preserved and it is dislocated from life position (fig. 6). In life the squamosal should contact the parietal posteromedially to form the lateral portion of the nuchal crest. A notch is developed along the dorsal edge of the squamosal portion of the nuchal crest (fig. 6). The posterior surface of the squamosal is smooth, but a cleft is developed on the dorsal edge between the posterior surface and the lateral side of the squamosal. A large and deep lateral recess makes up the entire lateral surface of the squamosal. The lateral recess is a feature observed only in derived troodontids such as *Gobivenator*, *Linhevenator*, and *Zanabazar* (Norell et al., 2009; Xu et al., 2011a; Tsuihiji et al., 2014). The lateral recess is rounded and relatively small in *Zanabazar*, but is triangular and proportionally large in *Almas ukhaa* and *Gobivenator* (Norell et al., 2009; Tsuihiji et al., 2014). The lateral recess of the squamosal is enclosed by curved anterior and posterodorsal walls, as well as a short ventral wall (fig. 6B). The posterodorsal wall also contributes to the posterior surface of the squamosal. The anterior wall and the posterodorsal wall define a short anterior process of the squamosal that projects anterodorsally. The anterior wall and the ventral wall meet antero-

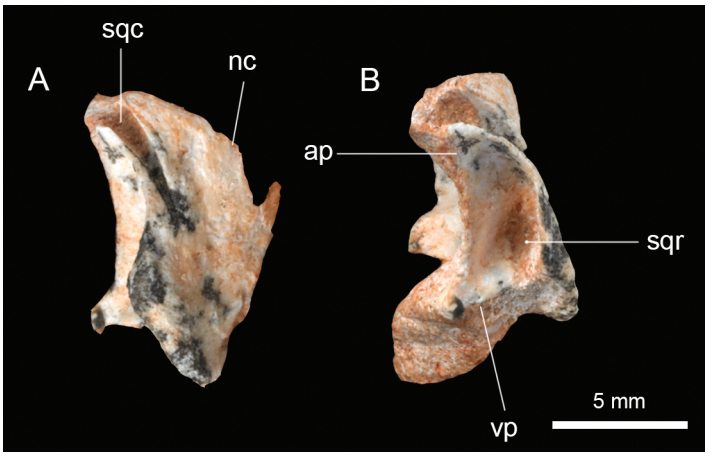

FIGURE 6. Left squamosal of IGM 100/1323 in **A.** posterolateral and **B.** lateral views.

ventrally and define a reduced ventral process of the squamosal. In this pattern, it is like *Gobivenator* and *Zanabazar* (Norell et al., 2009; Tsuihiji et al., 2014). In the basal troodontid *Sinovenator* (BMNHC 828), the lateral surface of the squamosal is concave but not as recessed as in more derived troodontids, and this recess is absent in dromaeosaurids and avialans.

Parietal: The parietals of IGM 100/1323 are exposed in ventral view (fig. 7A). The parietals are fused as is typical of most paravians except for some avialans. The anterior portion of the parietal is transversely more expanded than the posterior portion, which agrees with the pattern in *Mei*, *Gobivenator*, *Linhevenator*, *Zanabazar*, and *Troodon* (Currie 1985; Xu and Norell, 2004; Norell et al., 2009; Xu et al., 2011a; Tsuihiji et al., 2014), but differs from larger, derived dromaeosaurids such as *Velociraptor* and *Tsaagan* (Barsbold and Osmólska, 1999; Norell et al., 2006), in which the parietal is transversely more expanded on the posterior portion. The parietal is dorsally vaulted along the midline and descends laterally. The ventral surface of the parietal is smooth, but a transverse low ridge is developed ventrally at the most mediolaterally expanded position of the bone. The anterior edge of the parietal of the holotype appears U-shaped in ventral view, with the mid portion anteriorly convex. In contrast, the suture between the parietal and the frontal is W-shaped in *Mei* and *Gobivenator* (Xu and Norell, 2004; Tsuihiji et al., 2014). A small buttress is developed at the midline of the parietal-supraoccipital suture, probably as the extension of the sagittal crest of the parietal. A ramus extends posteroventrally from the posterior margin of the parietal (fig. 7A). It is anteroposteriorly compressed, and forms the medial portion of the nuchal crest on the occipital surface.

Pterygoid: The anterior end of the right pterygoid of IGM 100/1323 is exposed through the left antorbital fenestra (fig. 3). The anterior end of the pterygoid is straight and pointed as in other maniraptorans (Osmólska et al., 1972; Witmer; 1997; Mayr et al., 2007; Tsuihiji et al., 2014). The posterior portion of the left pterygoid is ventrally exposed (fig. 5). The posterior half of the pterygoid is slender, as in *Dromaeosaurus* and *Archaeopteryx* (Witmer, 1997; Mayr et al., 2007), but is not as broad as in *Saurornithoides* and *Gobivenator* (Norell et al., 2009; Tsuihiji et al., 2014). The pterygoid is ventrally concave. A short pterygoid flange curves pos-

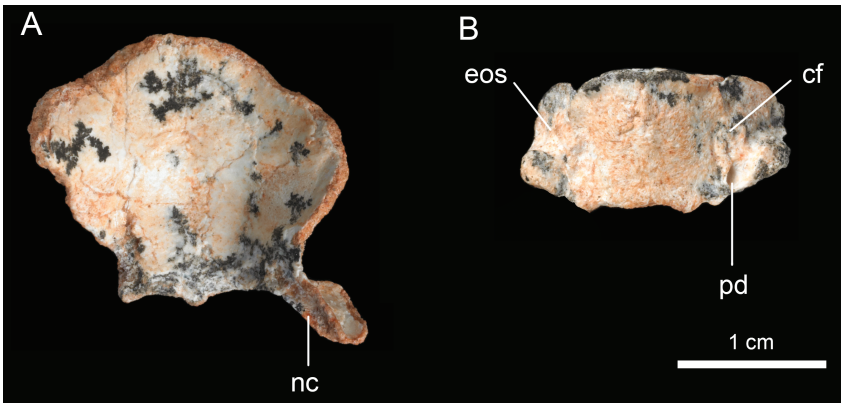

FIGURE 7. **A.** Parietal of IGM 100/1323 in ventral view; **B.** supraoccipital in posterior view.

teriorly, similar to the condition in *Dromaeosaurus* and *Archaeopteryx* (Witmer, 1997; Mayr et al., 2007), but different from that of *Saurornithoides* and *Gobivenator* (Norell et al., 2009; Tsuihiji et al., 2014), in which the pterygoid flange does not have posterior curvature. The sphenoid process of the pterygoid is located posteromedial to the pterygoid flange and articulates with the basipterygoid process of the parabasisphenoid. It is similar in size to the pterygoid flange and projects posteromedially.

Ectopterygoid: The left ectopterygoid of the holotype is dislocated and dorsally exposed (figs. 3, 5). As is typical of maniraptorans, the jugal process is slender and curved while the contact with the pterygoid is broad and sheetlike.

Sclerotic ring: Sclerotic rings are preserved in both orbits of the holotype (figs. 2, 3). The sclerotic ring is also observed in other paravians of various sizes, such as *Mei*, *Microraptor*, *Tsaagan*, and *Archaeopteryx* (Xu et al., 2003; Xu and Norell, 2004; Mayr et al., 2005; Norell et al., 2006; Schmitz and Motani, 2011). The best-exposed sclerotic plate seems nearly twice as long as wide and almost flat, as in *Tsaagan* (Norell et al., 2006). The sclerotic plates are relatively large in *Almas*, with a comparable size (relative to the orbit) to that of *Archaeopteryx* (Wellnhofer, 2009). A sclerotic ring has not been found in *Anchiornis* (Pei et al., 2017).

Braincase

The braincase of the holotype is shattered and laterally compressed, with most bones displaced. The supraoccipital, the left exoccipital/opisthotic, the prootic, and the parabasisphenoid appear unfused. In *Byronosaurus* the braincase is partially fused, with few sutures visible, whereas the braincases of *Saurornithoides*, *Zanabazar*, and *Sinovenator* are fully fused (Xu et al., 2002; Makovicky et al., 2003; Norell et al., 2009).

Supraoccipital: The supraoccipital is isolated from the rest of the cranium. The supraoccipital of *Almas ukhaa* is transversely broad and platelike, with the dorsal and ventral margins nearly parallel (fig. 7B), a feature observed in many paravians, such as *Gobivenator*, *Zanabazar*, and *Mahakala* (Norell et al., 2009; Turner et al., 2011; Tsuihiji et al., 2014). In derived drom-

aeosaurids such as *Tsaagan*, the supraoccipital is transversely narrow and triangular in posterior view (Norell et al., 2006). The posterior surface of the supraoccipital is convex along the midline. A weak axial nuchal crest is developed at the upper portion of posterior surface of the supraoccipital along the midline, becoming smooth at the lower portion (fig. 7B). The ventral edge of the supraoccipital (the dorsal margin of the foramen magnum) is sharp.

The supraoccipital bears a lateral wall (possibly the fused epiotic surface) on each side that expands anterolaterally (fig. 7B). The lateral wall of the supraoccipital likely sutures with the parietal, prootic, and laterosphenoid to form the dorsal wall of the braincase. A crescent-shaped fossa develops vertically where the posterior surface of the supraoccipital meets the anterolateral surface. Two foramina are present within the fossa, as in *Zanabazar* and *Troodon* (Currie and Zhao, 1993; Norell et al., 2009).

The supraoccipital is inflated ventral to the crescent-shaped fossa, and probably articulated with the exoccipital/opisthotic to form the posterodorsal wall of the otic capsule, as in *Troodon* (Currie and Zhao, 1993). The opening of a pneumatic duct is located medial to the lateroventral inflation of the supraoccipital as in *Troodon* (fig. 7B) (Currie and Zhao, 1993). In ventral view, the supraoccipital is thick laterally and forms the robust posterior wall of the otic capsule. A thick ridge develops along the medial surface of the supraoccipital, separating the braincase from the otic capsule.

Exoccipital/opisthotic: The left exoccipital/opisthotic of the holotype is preserved and exposed in posterior view (fig. 2). The exoccipital/opisthotic is displaced from its original position and its surface is weathered. The medial edge of exoccipital/opisthotic arcs and contributes to the lateroventral margin of the foramen magnum. The shape of foramen magnum cannot be directly observed, but considering the shape of supraoccipital and exoccipital/opisthotic, the foramen magnum is likely dorsoventrally long as in other troodontids (Makovicky and Norell, 2004).

The paroccipital process projects posterolaterally, as *Sinovenator*, *Troodon*, and some dromaeosaurids (Currie and Zhao, 1993; Xu et al., 2002; Norell et al., 2006), but differs from *Gobivenator*, *Byronosaurus*, and *Zanabazar*, in which the paroccipital process spreads laterally and does not evert posteriorly (Makovicky et al., 2003; Norell et al., 2009; Tsuihiji et al., 2014). The paroccipital process slightly curves dorsally, unlike typical theropods in which it is straight or ventrally curves. In *Byronosaurus* and *Gobivenator*, the distal end of the paroccipital processes curve slightly dorsally, as in *Almas ukhaa* (Makovicky et al., 2003; Tsuihiji et al., 2014). The posterior surface of the exoccipital/opisthotic is concave between the margin of foramen magnum and the paroccipital process, and the openings of CN X, XI, and XII are located in the concavity, which is typical of coelurosaurian dinosaurs. A rugose tubercle lateroventral to the foramen magnum is possibly the exoccipital contribution to the occipital condyle, like other maniraptorans and notably the Ukhaa perinate IGM 100/974 (Bever and Norell, 2009). A small ventral tab that represents the lateral portion of the basal tubera lies lateroventral to the foramen magnum, which indicates the occipital surface of *Almas ukhaa* is vertical as in *Byronosaurus*, *Zanabazar*, and *Troodon* (Currie and Zhao, 1993; Makovicky et al., 2003; Norell et al., 2009). In dromaeosaurids and the basal troodontid *Sinovenator*, the basal tubera is more anteriorly located (Xu et al., 2002). The ventral tab of the exoccipital/opisthotic bears a vertical

anterior surface in *Almas ukhaa*, which probably forms the posterior wall of a deep subotic recess that is also found in derived troodontids such as *Byronosaurus*, *Saurornithoides*, *Zanabazar*, and *Troodon* (Currie and Zhao, 1993; Makovicky et al., 2003; Norell et al., 2009). A deep subotic recess is convergent in ornithomimosaurs and derived troodontids. In the basal troodontid *Sinovenator*, the subotic recess is absent, and the ventral edge of the exoccipital/opisthotic lacks a vertical anterior surface.

Prootic: Both prootics of the holotype are dislocated from their original position (fig. 8). The left prootic is well preserved and resembles the prootic of IGM 100/974 (Bever and Norell, 2009). In lateral view, the prootic of *Almas ukhaa* has a typical troodontid profile as in *Sinovenator*, *Byronosaurus*, *Troodon*, *Saurornithoides*, *Zanabazar* and IGM 100/974 (Barsbold, 1974; Currie and Zhao, 1993; Xu et al., 2002; Makovicky et al., 2003; Norell et al., 2009, Bever and Norell, 2009). The paroccipital ramus of the prootic projects posterodorsally and forms a dorsal articulation with the exoccipital/opisthotic. The paroccipital ramus is short as in most troodontids such as *Byronosaurus* and IGM 100/974 (Makovicky et al., 2003; Bever and Norell, 2009), and not as elongate as in *Archaeopteryx* (Elżanowski, 2001). As in *Byronosaurus*, the paroccipital ramus of *Almas ukhaa* projects more laterally than that of IGM 100/974 (Makovicky et al., 2003; Bever and Norell, 2009). Anteriorly, the prootic articulates with the laterosphenoid. A saddle-shaped depression is located between the articular surface with the laterosphenoid and the paroccipital process, and represents the dorsal tympanic recess seen in many maniraptorans (Walker, 1985; Witmer, 1990; Xu et al., 2002), and notably the troodontids *Troodon*, *Byronosaurus*, and IGM 100/974 (Currie and Zhao, 1993; Makovicky et al., 2003). As in IGM 100/974 and *Archaeopteyrx* (Walker, 1985; Bever and Norell, 2009), the surface of the dorsal tympanic recess of *Almas ukhaa* is smooth and lacks a foramen (fig. 8), but a foramen is present in the dorsal tympanic recess of *Troodon* and *Byronosaurus* (Currie and Zhao, 1993; Makovicky et al., 2003). The posterior edge of the prootic forms the anterior margin of the middle-ear recess and the fenestra ovalis.

A depression lies ventral to the laterosphenoid contact. The anteromedial edge of the depression is arced and represents the posterior margin of the trigeminal fenestra (fig. 8). The opening of CN V is located anterior to the prootic and likely posteriorly defined by the laterosphenoid as in most deinonychosaurians, like *Byronosaurus*, *Troodon*, *Saurornithoides*, *Zanabazar, Velociraptor*, and *Dromaeosaurus* (Barsbold, 1974; Currie and Zhao, 1993; Makovicky et al., 2003; Norell et al., 2004; Norell et al., 2009). The opening of CN V is proportionally large in *Saurornithoides*, *Byronosaurus*, and *Almas ukhaa*, but in *Troodon* and *Zanabazar*, CN V is relatively small (Currie and Zhao, 1993; Makovicky et al., 2003; Norell et al., 2009). The ala parasphenoidalis develops ventral to the posterior margin of CN V, and is more prominent than that in IGM 100/974 (Bever and Norell, 2009). The ala parasphenoidalis has a flat and broad anterior surface, and contributes to the anterior part of the otosphenoidal crest (fig. 8).

A small foramen develops posteroventral to the exit of CN V on the lateral side of the prootic, representing the opening of CN VII (fig. 8). The anterior tympanic crista is located ventral to CN VII, which represents the dorsal/posterodorsal portion of the otosphenoidal crest. The otosphenoidal crest defines a pneumatic lateral depression of the braincase and is

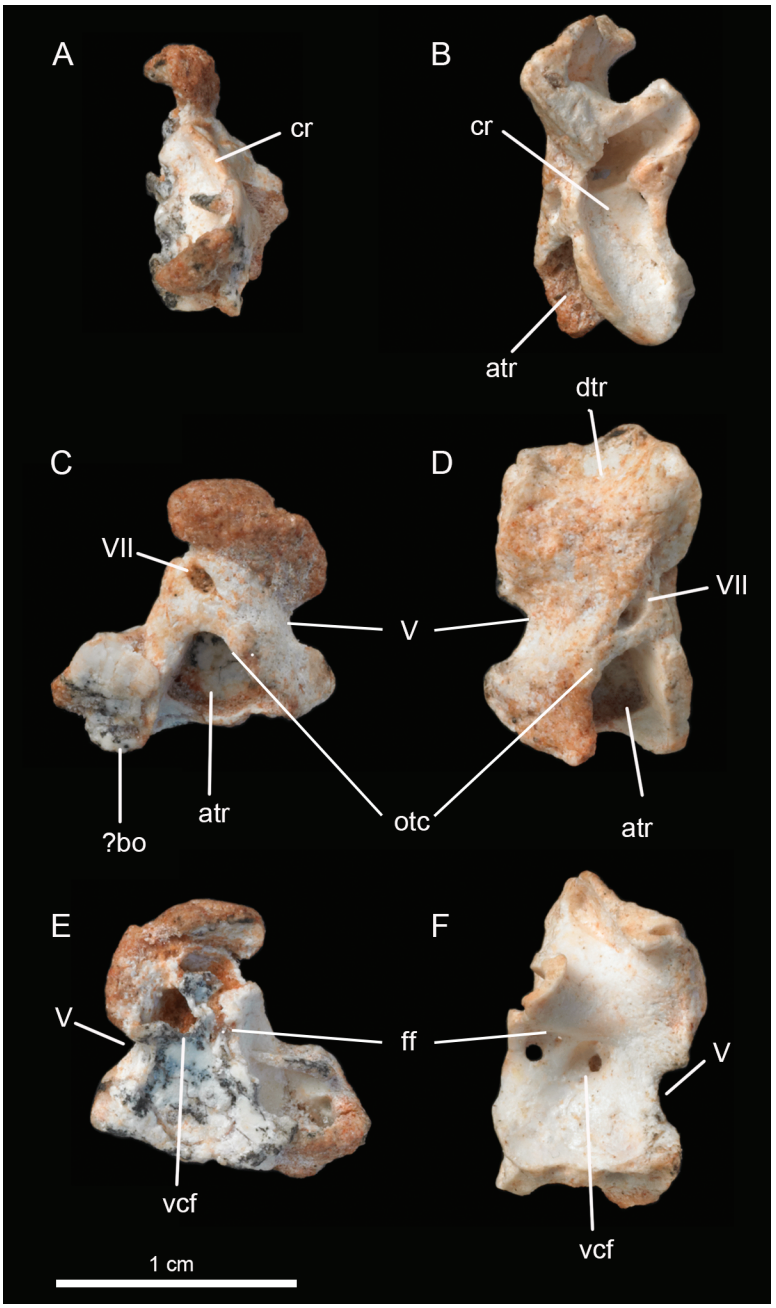

FIGURE 8. Prootic of IGM 100/1323. Right prootic in **A.**anterior, **C.** lateral and **E.** medial views; left prootic in **B.** anterior, **D.** lateral, and **F.** medial view.

present in derived troodontids (Currie and Zhao, 1993; Makovicky et al., 2003; Norell et al., 2009). A similar structure develops in the Ukhaa perinate IGM 100/974, but the otosphenoidal crest is not as distinct as in *Almas ukhaa*. As in *Byronosaurus*, *Saurornithoides*, and IGM 100/974, CN VII is located posterodorsal to the pneumatic lateral depression in *Almas ukhaa* (Makovicky et al., 2003; Norell et al., 2009). In contrast, CN VII of *Troodon* and *Zanabazar* is located within the pneumatic lateral depression (Barsbold, 1974; Currie and Zhao, 1993; Norell et al., 2009). The prootic surface between CN VII and the anterior tympanic crista is smooth, as in *Byronosaurus* and *Saurornithoides*, but it lacks the rugose texture observed in the Ukhaa perinate IGM 100/974 (Makovicky et al., 2003; Norell et al., 2009), perhaps indicative of a more advanced ontogenetic stage.

A large and distinct anterior tympanic recess develops ventral to the anterior tympanic crista and it opens lateroventrally (fig. 8). The anterior tympanic recess of *Almas ukhaa* is deep and large, and makes up most of the lateral depression as in *Troodon, Zanabazar*, and *Saurornithoides* (Currie and Zhao, 1993; Makovicky et al., 2003; Norell et al., 2009). This differs from IGM 100/1126 and *Byronosaurus*, in which the lateral depression is shallow and the anterior tympanic recess is more anteriorly located (Makovicky et al., 2003). In the Ukhaa perinate IGM 100/974, the anterior tympanic recess is represented by a socket ventral to CN VII (Bever and Norell, 2009), similar to *Almas ukhaa, Troodon*, and *Saurornithoides*, but it is proportionally smaller, possibly reflecting ontogenetic or allometric variation in troodontid dinosaurs. The medial wall of the anterior tympanic recess of *Almas ukhaa* is prominent in as in *Troodon* and *Saurornithoides* (Currie and Zhao, 1993; Norell et al., 2009), but different from IGM 100/974, in which the medial wall of the anterior tympanic recess is only weakly developed. A foramen is located deep inside the anterior tympanic recess. A triangular fossa develops at the posteroventral corner of the anterior tympanic recess, and on the posterior wall of the lateral depression. A similar fossa is also observed in *Saurornithoides*, yet is absent in *Byronosaurus* (see Makovicky et al., 2003; Norell et al., 2009).

Posteriorly, a longitudinal canal runs along the anterior wall of the cochlear recess as in IGM 100/974 (fig. 8). The medial surface of the prootic of *Almas ukhaa* is similar to that of IGM 100/974, except that the anterior tympanic recess is medially obfuscated by the lateral wall of the braincase. The prootic of *Almas ukhaa* has a straight ventral edge. An acoustic recess is located in the middle of the medial surface of the prootic in the holotype of *Almas ukhaa*, like that observed in IGM 100/974 (Bever and Norell, 2009). The facial fossa and vestibulocochlear fossa are located within the acoustic recess, which is widely observed in theropods and here confirmed as present in the troodontid *Byronosaurus* and IGM 100/974 (Makovicky et al., 2003; Bever and Norell et al., 2009).

The vestibule-cochlear fossa is penetrated by two foramina that transmit branches of CN VIII into the inner ear (fig. 8). The vestibular foramen is positioned above the cochlear foramen at the anterior margin of the vestibulocochlear fossa. The vestibular foramen transmits the vestibular branch of CN VIII, and it opens onto the floor of the vestibule. As in IGM 100/974, the cochlear foramen of the vestibulocochlear fossa is larger than the vestibular foramen, and it opens medioventrally into the anterior wall of the cochlear recess. The facial fossa is located anterior to the

vestibulocochlear fossa (fig. 8). Unlike IGM 100/974, a small foramen located ventrally in the facial fossa opens into the anterior tympanic recess, which may be homologous to the pneumatic recess lying in the anterior tympanic recess of *Troodon* (Currie and Zhao, 1993).

The dorsal portion of the right prootic is damaged, and the morphology of the remaining portion is identical to the left prootic.

Basioccipital: A fragmentary bone possibly representing a partial basioccipital articulates with the right prootic posterior to the lateral depression of the braincase (fig. 8). This element forms a convex surface posteroventral to the lateral depression of the braincase and anteroventral to the middle-ear recess. In *Saurornithoides* and *Byronosaurus*, a similar convex surface is present between the lateral depression, the middle-ear recess and the subotic recess (Makovicky et al., 2003; Norell et al., 2009). The subotic recess cannot be directly observed in the holotype, but this fragmentary element may contribute to the anterolateral wall of the subotic recess as in *Byronosaurus* and *Saurornithoides* (Makovicky et al., 2003; Norell et al., 2009).

Parabasisphenoid: The parabasisphenoid of the holotype is preserved, but the surface of the bone is eroded (fig. 2). The basipterygoid process of the parabasisphenoid directs anteroventrally as in the basal troodontid *Sinovenator* (Xu et al., 2002). The basipterygoid process of *Almas ukhaa* is hollow as in derived troodontids such as *Byronosaurus* and *Troodon*, and it is anteroposteriorly broad as in *Troodon* (Currie and Zhao, 1993; Makovicky et al., 2003). In contrast, the basisphenoid process is solid in *Sinovenator* (Xu et al., 2002).

A dorsoventrally deep cultriform process projects horizontally in *Almas ukhaa*, as in *Troodon*, but proportionally larger and deeper than that in *Byronosaurus* and *Sinovenator* (Currie and Zhao, 1993; Xu et al., 2002; Makovicky et al., 2003). The lateral surface of the parasphenoid bulla is not recessed (fig. 2). This is similar to *Troodon* and *Sinovenator*, but differs from that of *Byronosaurus* and IGM 100/1126 (Currie and Zhao, 1993; Xu et al., 2002; Makovicky et al., 2003). The parasphenoid bulla bears a longitudinal groove dorsally, and the hypophyseal fossa is located at the posterior part of the parasphenoid bulla within the dorsal groove. The hypophyseal fossa of *Almas ukhaa* is shallow and not as developed as in *Troodon*, but similar to that of *Sinovenator* (Currie and Zhao, 1993; Xu et al., 2002).

Mandible: The anterior portions of both dentaries are preserved in IGM 100/1323 (figs. 2, 4). The symphyseal region of the dentary is straight laterally, unlike the medially curved dentary observed in derived troodontids like *Saurornithoides* and *Zanabazar* (Norell et al., 2009). This condition approximates that of *Sinovenator*, *Byronosaurus*, and *Sinornithoides* (Russell and Dong, 1993; Xu et al., 2002; Makovicky et al., 2003). The anterior portion of the dentary has relatively parallel dorsal and ventral edges as in most paravians. The lateral surface of the anterior portion of the dentary is smooth, similar to the Ukhaa perinate IGM 100/974, but does not bear a lateral groove that is characteristic of other troodontids and some other paravians (figs. 2, 4) (Makovicky and Norell, 2004; Makovicky et al., 2005; Turner et al., 2012). The lateral groove usually becomes more distinct at the posterior part of the dentary in other troodontids, such as *Sinovenator*, *Jianianhualong*, and *Zanabazar* (Xu et al., 2002; Norell et al., 2009; Xu et al., 2017), but whether the dentary of *Almas ukhaa* has a posteriorly distinct groove

is unknown, as the posterior part of the dentary is missing. A deep Meckelian groove is observed medially on the left dentary of the holotype. The splenial of *Almas ukhaa* is elongate and attaches medially to the dentary, ventral to the Meckelian groove.

The anterior end of the dentary toothrow is slightly downturned, and the first two tooth positions are not strictly in the same plane as the rest part of the toothrow (figs. 2, 4). A similar condition is observed in many maniraptorans, such as *Anchiornis*, *Microraptor*, and *Byronosaurus* (Makovicky et al., 2003; Pei et al., 2014). Twenty-three tooth positions are observed on the preserved portion of the left dentary. The dentary teeth of *Almas ukhaa* are more closely packed anteriorly than posteriorly as is typical for troodontids. The anterior teeth are about the same size as the middle ones. The dentary teeth have the same morphology as the maxillary teeth. They recurve slightly, and constrict between the crown and the root. The dentary teeth lack serrations. As in most other troodontids, with the exception of *Urbacodon* (Makovicky et al., 2003; Averianov and Sues, 2007; Bever and Norell, 2009), the dentary teeth rest in an open groove along the dorsal edge of the dentary and the toothrow lacks visible interdental plates.

Some postdentary bones on the left mandible are partially exposed (figs. 2, 3, 4). As is typical of paravians, the surangular is laterally ridged on the dorsal edge. The dorsal surface of the surangular is faced dorsolaterally as in many troodontid and dromaeosaurid dinosaurs (figs. 3, 5). The triangular tab, which defines the glenoid fossa anteriorly, projects laterally in *Almas ukhaa* along the dorsolateral ridge of the surangular. A single distinct oval surangular foramen penetrates the mandible anteroventral to the glenoid fossa (figs. 3, 5). The surangular foramen is anteroposteriorly elongate as in *Xiaotingia* and *Anchiornis* (Hu et al., 2009; Xu et al., 2011b), but differs from the rounded foramen of *Tsaagan* (Norell et al., 2006). The retroarticular process flattens dorsoventrally in *Almas ukhaa*. It lacks a vertical column, or spike, that is typical of dromaeosaurid dinosaurs (fig. 3).

Postcranium

Sacral vertebrae: Three sacral vertebrae are preserved (fig. 9). The centra of the sacral vertebrae remain unfused, which may indicate a preadult ontogenetic stage of the holotype. The centra of the sacral vertebrae are transversely wide. The posterior sacral centrum (possibly the fifth) is smaller than the centra of the middle sacral vertebrae (possibly the third and the fourth) This condition is similar to *Zanabazar* and *Sinovenator* (Xu et al., 2002; Norell et al., 2009), but different from *Saurornithoides* and *Velociraptor* (Norell and Makovicky, 1997; Norell et al., 2009), in which the size of the sacral vertebrae are relatively constant. The sacral region of the holotype is heavily eroded, thus more detailed information is not available.

Caudal vertebrae: Eleven proximalmost caudal vertebrae are preserved in the holotype, whereas the more distal caudal vertebrae are missing (figs. 9–11). The first five caudal vertebrae are closely packed, and the sixth to the 11th preserved caudal vertebrae are associated. The centra of the first and the 11th caudal vertebrae are missing.

The centra of the second to the eighth caudal vertebrae have similar size. They are anteroposteriorly short, as is typical of paravians. The centrum of the ninth preserved caudal is elon-

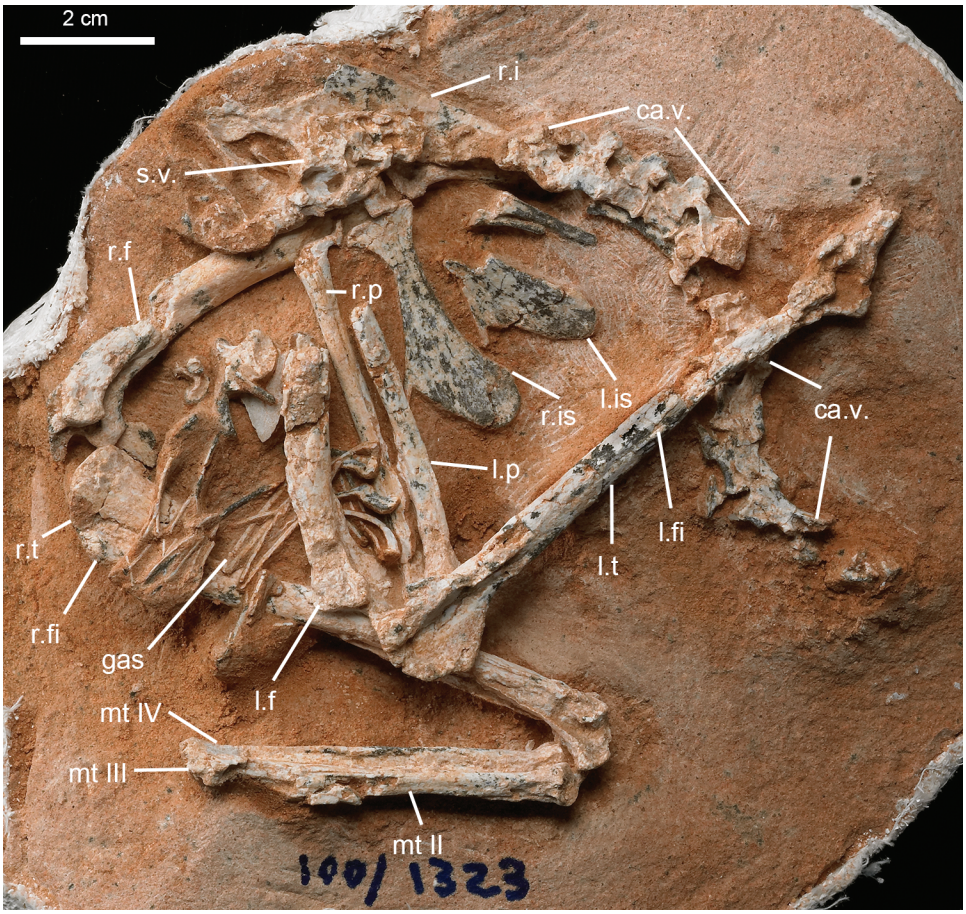

FIGURE 9. Postcranium of IGM 100/1323.

gate, and is 1.5× as long as the second caudal centrum. This matches the pattern seen in other troodontid dinosaurs in which the elongation of the caudal vertebrae happens around the 10th caudal vertebra (Makovicky and Norell, 2004). The centrum of the 10th caudal vertebra is only partially preserved and more posterior centra are missing. All the preserved centra have ventral keels and are slightly concave along the ventral surface, which is similar to *Sinovenator*, *Mei*, *Sinornithoides*, *Gobivenator*, and *Saurornithoides*, but unlike *Zanabazar*, in which the centra are ventrally smooth (Currie and Dong, 2001; Xu et al., 2002; Xu and Norell, 2004; Norell et al., 2009; Tsuihiji et al., 2014).

The neural arches are relatively tall on the first five exposed caudal vertebrae, almost twice as high as the corresponding centra (fig. 10). The neural spine is rectangular and inclines posterodorsally. The postzygapophyses are developed posterolateral to the neural spine. The prezygapophyses are slender, and abut the preceding postzygapophyses lateroventrally. As in *Saurornithoides*, the prezygapophyses can reach about one-third the length of the preceding caudal centra (Osborn, 1924; Norell et al., 2009). The bases of the prezygapophyses are more ventrally placed than the postzygapophyses. The transverse processes on the anterior vertebrae are severely

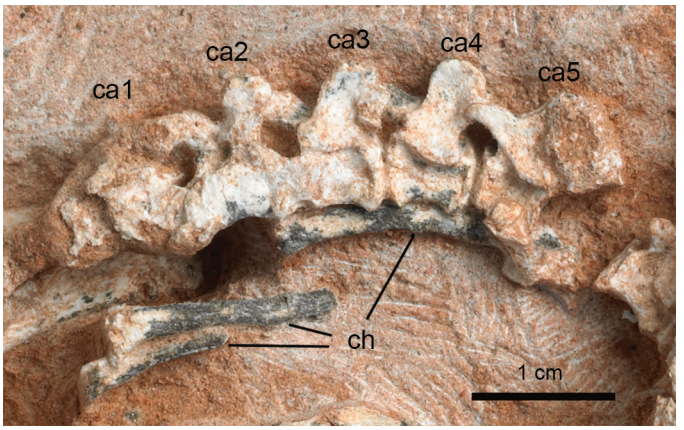

FIGURE 10. Proximal caudal vertebrae of IGM 100/1323.

eroded, whereas distinct and posterolaterally directed transverse processes are observed on the fourth and fifth caudal vertebrae (fig. 10). Troodontids typically have an elongate and slender transverse process on the anteriormost caudal vertebrae (Xu, 2002; Makovicky and Norell, 2004). The neural arches and the neural spines are reduced from the sixth to the 10th vertebrae (fig. 11). The prezygapophyses of the sixth to the 10th vertebrae can reach no more than one-fourth the length of the more anterior centrum, relatively shorter than in the basal troodontid *Sinovenator* (Xu et al., 2002). The transverse processes are represented only by faint ridges on the sixth to 10th caudal vertebrae. The neural arches are partially fused with the centra in *Almas ukhaa*.

The first three preserved chevrons are elongate (fig. 10). The first chevron is about 1.5× the length of the first caudal vertebra. The following two chevrons increase in length. The third chevron of *Almas ukhaa* reaches the maximum length, and is more than 3× as long as the corresponding caudal vertebrae, which is unique in all troodontids. The elongation of chevrons is a primitive condition in coelurosaurians, but is also observed in derived troodontids such as *Saurornithoides*, *Gobivenator*, and *Sinornithoides.* In *Saurornithoides* and *Gobivenator*, the longest chevron is about 2–2.5× the length of the corresponding caudal vertebra (see Norell et al., 2009; Tsuihiji et al., 2014). The chevrons of *Almas ukhaa* are proportionally longer than those in these derived troodontid taxa. The chevrons preserved under the sixth to 10th caudal vertebrae are reduced and become anteroposteriorly elongate, as is typical of paravians, such as *Zanabazar* and *Sinornithoides* (Currie and Dong, 2001; Norell et al., 2009)

Gastralia: The posterior elements of the gastralia are preserved in IGM 100/1323 (fig. 9). The medial segments of the gastralia abut each other and form a basketlike structure as in most other theropod dinosaurs (Claessens, 2004). This pattern is also observed in other deinonychosaurians such as *Mei*, *Sinornithoides*, *Velociraptor*, and *Microraptor* (Norell and Makovicky, 1997; Currie and Dong, 2001; Hwang et al., 2002; Xu and Norell, 2004; Pei et al., 2014). The posteriormost gastral elements approach the pubic apron in the holotype. They are curved and bear a robust hooklike structure distally as in *Gobivenator* (Tsuihiji et al., 2014).

Ilium: The right ilium of the holotype is mostly preserved and exposed in medial view, while the anterodorsal part of the ilium is damaged (fig. 9). As in all paravians, the ilium is

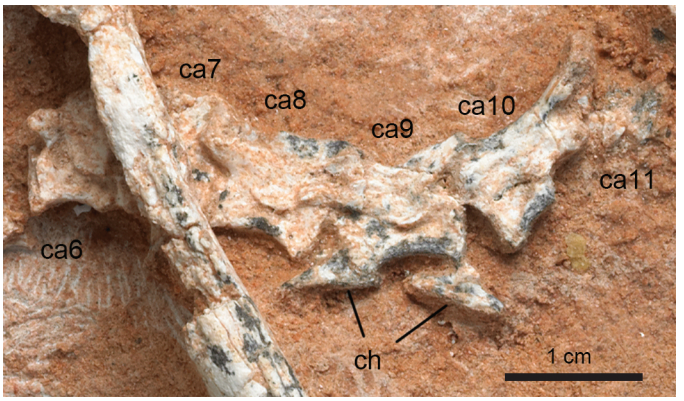

FIGURE 11. Proximal and middle caudal vertebrae of IGM 100/1323.

dolichoiliac and dorsoventrally shallow in lateral view. The anterior process of the ilium is slightly shorter than the posterior process, which is common in nonavian paravians (Turner et al., 2011). The anterior tip of the anterior process is rounded, slightly ventrally directed as is typical of paravians, and much like the profile of *Anchiornis* and *Mahakala* (Hu et al., 2009; Turner et al., 2011). The anterior tip of the anterior process lacks a pointed hook that is typical of primitive coelurosaurians, similar to *Mei*, *Gobivenator*, and *Mahakala* (Xu and Norell, 2004; Turner et al., 2011; Tsuihiji et al., 2014). The ventral edge of the anterior process is sharp and curved in *Almas ukhaa*, though not as curved as in *Sinusonasus* (Xu and Wang, 2004).

The posterior process of the ilium of *Almas ukhaa* directs horizontally, with the ventral edge slightly curved and thickened near the ischiadic peduncle (fig. 9), which is similar to the condition of *Gobivenator*, *Sinovenator*, *Mei*, *Jinfengopteryx*, *Anchiornis*, and *Archaeopteryx* (Ostrom, 1976; Xu et al., 2002; Xu and Norell, 2004; Ji and Ji, 2007; Tsuihiji et al., 2014). Typically, the posterior process of the ilium in dromaeosaurids is more ventrally curved posteriorly compared to troodontids, as in *Mahakala*, *Velociraptor*, and *Microraptor* (Norell and Makovicky 1997; Hwang et al., 2002; Turner et al., 2007b; Pei et al., 2014). The dorsal edge of the ilium is convex and sharpens posteriorly. A brevis shelf is observed on the medial side of posterior process of the ilium, for the attachment of transverse processes of the posterior sacral vertebrae. The brevis shelf projects from the posterior edge of the ischiadic peduncle and ends medial to the posterior end of the iliac blade.

Ventrally, the pubic and the ischiadic peduncles of *Almas ukhaa* are similar in size (fig. 9). The pubic peduncle is mostly obfuscated by the sacrum and not completely visible in medial view. The ischiadic peduncle of *Almas ukhaa* is triangular in medial view. It is anteroposteriorly long and posteriorly centered as in *Sinovenator* and *Mahakala* (Xu, 2002; Turner et al., 2007b; Turner et al., 2011). The medial surface of the ischiadic peduncle is concave. The acetabulum of *Almas ukhaa* is wider than deep, inferred from the shape of the ischiadic peduncle, as in *Sinovenator* and *Gobivenator* (Xu et al., 2002; Tsuihiji et al., 2014).

Pubis: Both pubes of the holotype are preserved (fig. 12), except for the proximal end of the left pubis. The pubis is dislocated from the ilium, and it is possibly anteroventrally posi-

FIGURE 12. Pubes of IGM 100/1323.

tioned, as inferred from the shape of the articular facet with the ischium. The anteroventral orientation of the pubis is a derived state observed in derived troodontids, in contrast to a posteroventral condition observed in basal paravians such as *Sinovenator*, *Unenlagia*, *Sinornithosaurus*, *Rahonavis*, and *Archaeopteryx* (Novas and Puerta, 1997; Xu et al., 1999; Xu et al., 2002; Wellnhofer, 1974; Forster et al., 1998), and the fully backward oriented condition of most dromaeosaurids and derived avialans (Norell and Makovicky, 2004). The pubic shaft is 1.56× the length of the ischium (see table 1). It is rodlike proximally and anteroposteriorly flattened distally. A longitudinal groove is developed along the medial side of the pubic shaft. A similar groove is also observed in *Sinovenator* (Xu, 2002). Laterally, the pubic shaft is straight, and becomes ridged posterolaterally below the pubic apron. The pubis of *Almas ukhaa* lacks the lateral tubercle that is present in *Sinovenator* and microraptorians (Xu et al., 2002; Hwang et al., 2002; Pei et al., 2014). This tubercle is not present in derived troodontids and other dromaeosaurids (e.g., Norell and Makovicky, 1997; Zanno et al., 2011, Tsuihiji et al., 2014). The pubic shaft of *Almas ukhaa* is straight in lateral view as in *Gobivenator*, *Talos*, *Saurornithoides*, *Sinornithoides*, and *Troodon* (Russell and Dong, 1993; Norell et al., 2009; Zanno et al., 2011; Tsuihiji et al., 2014), but unlike the posteriorly curved pubis of other paravians (e.g., Hwang et al., 2002; Foth et al., 2014). The pubic apron begins at the distal two-fifths of the shaft (fig. 9), much shorter than that of *Sinovenator* (Xu et al., 2002). The pubic apron remains unfused in *Almas ukhaa* and the pubic apron diminishes in width as it projects ventrally, and probably leaves an open slit along the midline distally, as is observed in most other deinonychosaurians (Xu et al., 2002; Norell and Xu, 2004). The distal end of the pubis is anteroposteriorly expanded. A triangular pubic boot is present. It expands more anteriorly than posteriorly. In contrast, the pubic boot is posteriorly expanded in *Unenlagia*, *Sinovenator*, and *Anchiornis* (Novas and Puerta, 1997; Xu et al., 2002; Pei et al., 2017), but is expanded both anteriorly and posteriorly in many derived troodontids and some dromaeosaurids (Barsbold, 1983; Tsuihiji et al., 2014).

Ischium: The right ischium of the holotype is completely preserved, but only the distal half of the left is preserved (fig. 13). The ischium is about 63% the length of the pubis, comparatively longer than in *Sinovenator* and *Mei* (Xu et al., 2002; Xu and Norell, 2004), but close to the condition of *Gobivenator* and *Talos* (Zanno et al., 2011; Tsuihiji et al., 2014). As in most maniraptorans the ischia of *Almas ukhaa* are not fused distally, but unlike *Saurornithoides* and many oviraptorosaurs (Norell et al., 2009; Balanoff and Norell, 2012), in which the ischia are fused. The proximal end of the ischium is expanded. A shallow notch separates the pubic peduncle and the iliac peduncle of the ischium proximally, which is similar to *Sinovenator* (Xu et al.,

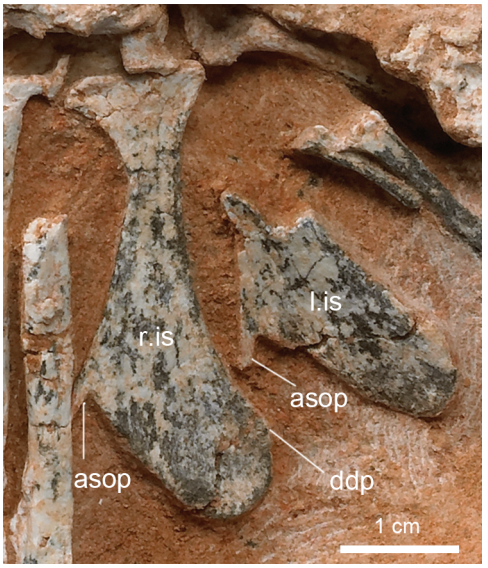

FIGURE 13. Ischia of IGM 100/1323.

2002). This notch is more deeply defined in *Gobivenator* and *Talos* (Zanno et al., 2011; Tsuihiji et al., 2014). A constriction is present ventral to the proximal end, in which the ischiadic shaft of *Almas ukhaa* is constricted to half the width of the proximal end (fig. 13). The ischiadic shaft is mediolaterally flat. The obturator process is developed on the anterior edge of the ischium, and located on the distal one-third of the pubic shaft. This condition differs from *Gobivenator*, *Sinornithoides*, *Saurornithoides*, and *Talos*, in which the obturator process is located close to the midshaft of the ischium (Russell and Dong, 1993; Norell at al., 2009; Zanno et al., 2011; Tsuihiji et al., 2014). A distinct spikelike process extends ventrally from the anterior edge of the obturator process in *Almas ukhaa* (fig. 13). This is a very unusual feature and expressed to a degree not seen in any other dinosaurs. A similar structure is also observed in *Gobivenator* (Tsuihiji et al., 2014), but is proportionally shorter than in *Almas ukhaa*. In *Saurornithoides*, the anterior edge of the obturator process is ridged, but lacks a spikelike anteroventral process (Osborn, 1924; Norell et al., 2009).

The distal one-third of the posterior ischiadic shaft is posteriorly curved in the holotype, while the proximal two-thirds of the shaft appears straight. The distal end of the ischium is expanded and lobe shaped in lateral view (fig. 13), like that in the unnamed troodontid IGM 100/1126, but unlike the bladelike distal ischium of *Gobivenator*, *Saurornithoides*, *Linhevenator*, and *Talos* (Norell et al., 2009; Zanno et al., 2011; Xu et al., 2011a; Tsuihiji et al., 2014), and the shortened ischium of *Sinovenator*, *Jinfengopteryx*, and *Anchiornis* (Xu et al., 2002; Ji et al., 2005; Xu et al., 2008). The posterior edge of the ischiadic blade of *Almas ukhaa* is smooth and lacks the well-defined proximal dorsal process observed in *Sinovenator* and *Gobivenator* (Xu et al., 2002; Tsuihiji et al., 2014). A small triangular tab close to the distal end of the ischiadic blade may represent the distal dorsal process. The ischiadic shaft is laterally convex and the medial surface of the ischium of *Almas ukhaa* is flat.

Hind Limb

The surface of the hind-limb bones is rugose, which may or may not be periosteal surface texture, perhaps indicating immaturity. However, a rugose surface is known to occur in some other adult deinonychosaurians (Csiki et al., 2010; Brusatte et al., 2013). The surface texture of the hind limb is hard to determine due to erosion.

Femur: Both femora are preserved. The right femur is broken into two parts and exposed in medial view, and only the distal half of the left femur is preserved (fig. 9). The skull/femur

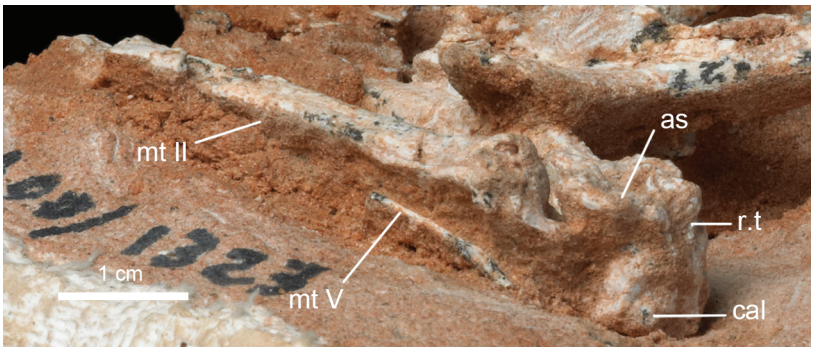

FIGURE 14. Right ankle of IGM 100/1323 in distal view and right pes in posterior view.

length ratio of *Almas ukhaa* (~1.2) is higher than other troodontids of comparable size (*Mei* and *Sinovenator*, both within a range of 0.8–1.1). A relatively high skull/femur length ratio (~0.95) is also observed in the larger-bodied *Gobivenator* (Tsuihiji et al., 2014). Though a larger cranial size is usually associated with immaturity, whether the high skull/femur ratio in *Almas* is solely related to ontogeny cannot be determined until more specimens are discovered.

The femur is slightly bowed as is typical of theropods (Gauthier, 1986). Proximally, the femur is not well exposed. A ridgelike longitudinal posterior trochanter develops on the posterior surface of the femur, as in the derived troodontids such as *Talos*, *Linhevenator*, *Philovenator*, and *Saurornithoides* (Norell et al., 2009; Zanno et al., 2011; Xu et al., 2011a; Xu et al., 2012). Distally, both the lateral and medial condyles of the femur project posteriorly. The lateral condyle appears more posteriorly extended than the medial condyle on the right femur while the medial condyle is more posteriorly extended on the left femur, and this variation is likely a preservational bias. A deep and distally open popliteal fossa is present posteriorly, defined between the posterior ridges of the medial and lateral condyles (fig. 9). As is typical of paravians, the distal lateral condyle of the femur is transversely wider than the medial condyle, and the posterior ridge of the lateral condyle is more prominent than that of the medial condyle. A weak supracondylar crest is developed on the posterior edge of the lateral condyle of *Almas ukhaa* (fig. 9). Unlike *Byronosaurus*, it lacks a notch that separates the supracondylar crest from the lateral condyle. An eroded ectepicondyle is developed on the medial condyle of the femur of the holotype anteriorly.

Tibia: Both tibiae are almost completely preserved, with only slight erosion on the surface (fig. 9). The tibia is about 1.4× the length of the femur, which is comparable to that of *Sinovenator*, *Mei*, and *Anchiornis* (Xu et al., 2002; Xu and Norell, 2004; Pei et al., 2017). The tibial shaft is straight and round in cross section. The proximal end of the tibia expands anteriorposteriorly. A prominent cnemial crest rises anteromedially on the proximal end of the tibia. The proximal edge of the cnemial crest slopes anteroventrally in lateral view, resembling the condition of *Gobivenator* (Tsuihiji et al., 2014), but different from that of *Byronosaurus* (Makovicky et al., 2003). A moderately developed fibular condyle on the proximal tibia contacts the fibula (fig. 9). A wide groove is developed between the cnemial crest and the lateral crest on the holotype. The posterior condyle of the proximal tibia is confluent with the dorsal edge of

the bone and posteriorly overhangs the tibial shaft as in *Byronosaurus* and *Bambiraptor* (Burnham et al., 2000; Makovicky et al., 2003). The proximal medial condyle of the tibia is weakly developed in *Almas ukhaa*.

Distal to the cnemial crest, an anterior ridge is developed on the anterior surface of the tibia. This ridge forms between the anterior and medial faces of the tibial shaft. This ridge reaches the midpoint of the tibia, and then becomes flat distally. This condition is similar to *Sinovenator* and *Mahakala* (Xu et al., 2002; Turner et al., 2011). Distally, the end of the tibia expands mediolaterally. The right tibia is not fused with the astragalus and the calcaneum, but whether the tarsals were fused to the left tibia cannot be determined due to erosion (fig. 14).

Fibula: The right fibula is eroded and only its partial proximal end and a small portion of the mid shaft are preserved, whereas the left fibula has portions of its distal end preserved (fig. 9). The proximal end of the fibula is expanded and bears a prominent crest posteriorly. The fibula is extremely slender distally, and its distal end probably attaches anterolaterally on the tibiotarsus.

Tarsals: The astragalus and calcaneum are cofused as in *Gobivenator* and *Philovenator* (fig. 14) (Xu et al., 2012; Tsuihiji et al., 2014). The proximal tarsals direct anteroventrally on the distal end of the tibia in *Almas*, and project more ventrally than in IGM 100/1126, *Talos*, and *Zanabazar* (Norell et al., 2009; Zanno et al., 2011). The astragalus is hourglass shaped in distal view. The ascending process of the astragalus is triangular and high, and the center is medial to the tibiotarsus midline. This is typical of most coelurosaurians (Zanno et al., 2011). A shallow but wide groove is developed between the distal condyles of the tibiotarsus anteroventrally. In *Almas ukhaa*, the suture between the astragalus and the tibia is distally exposed on the tibiotarsus, as also observed in *Zanabazar* and *Talos* (Norell et al., 2009; Zanno et al., 2011).

FIGURE 15. Right pes of IGM 100/1323 in anterior view.

TABLE1. Selected Measurements (in mm) of IGM 100/1323.

Skull length	~82
Skull height	35.3
Left ilium	56.5
Left pubis	60.1
Right ischium	38.5
Right femur	68.3
Right tibiotarsus	94.5
Left tibiotarsus	96.1

Pes: The right metatarsus is partially preserved, with only the distal end missing (figs. 9, 14). The proximal end of metatarsal IV is preserved on the left side (fig. 9). The metatarsus of *Almas ukhaa* is fully arctometatarsalian as in derived troodontids, with metatarsal III strongly pinched between metatarsals II and IV (Makovicky and Norell, 2004).

Metatarsal II is proximally expanded, but it is mediolaterally compressed along the shaft distally (fig. 15). Metatarsal II is less robust than metatarsal IV, which agrees with the asymmetric metatarsi of troodontid dinosaurs (Makovicky and Norell, 2004). In *Almas ukhaa*, the shaft of metatarsal II is less than 50% the width of metatarsal IV, as in *Talos*, *Tochisaurus*, *Gobivenator*, *Troodon*, *Philovenator*, *Linhevenator*, *Saurornithoides*, and IGM 100/1126 (Wilson and Currie, 1985; Kurzanov and Osmólska, 1991; Norell et al., 2009; Zanno et al., 2011; Xu et al., 2011a; Tsuihiji et al., 2014). In *Jinfengopteryx*, *Sinovenator*, *Mei*, *Jianianhualong*, *Sinusonasus*, IGM 100/44, and *Sinornithoides*, the shaft of metatarsal II is nearly as wide as metatarsal IV (Barsbold et al., 1987; Currie and Dong, 2001; Xu et al., 2002; Xu and Norell, 2004; Xu and Wang, 2004; Ji and Ji, 2007; Xu et al., 2017). The proximal end of metatarsal II is more medially expanded, and reaches the proximal end of metatarsal IV as in other derived troodontids (Kurzanov and Osmólska, 1991; Zanno et al., 2011; Tsuihiji et al., 2014).

Metatarsal III is strongly constricted in a groove formed between metatarsals II and IV and is not visible proximally on the anterior surface (fig. 15). Metatarsal III has an anterior exposure from only distal to the mid portion of the metatarsus. As in derived troodontids (e.g., *Troodon*, *Gobivenator*, *Talos*, *Philovenator*, *Linhevenator*, and *Tochisaurus*), the proximal shaft of metatarsal III is strongly pinched compared with its distal shaft in anterior view, which makes the proximal one-third of the shaft either not exposed or less than 25% the width of the distal one-third of the shaft on the anterior surface. In contrast, in *Sinovenator* and *Sinusonasus* the proximal shaft of metatarsal III is not as strongly pinched as in *Almas* and has a width around half of that of the distal one-third of the shaft. The preserved distal portion of metatarsal III appears symmetric, with equal expansion on each side.

Metatarsal IV is significantly more robust than metatarsal II (fig. 15). It is dorsoventrally deeper than transversely wide, which is typical of derived troodontids, but different from *Sinovenator* (Xu et al., 2002). Metatarsal IV also thins distally, but remains transversely wider than

metatarsal II. The anterior surface of metatarsal IV is proximally broad and becomes a prominent ridge on the mid and distal shaft.

The spikelike metatarsal V is much more slender and less than one-third the length of metatarsals II, III, and IV (fig. 14). It attaches posteriorly on metatarsal IV. Metatarsal V is straight as in *Sinornithoides*, in contrast to the curved metatarsal V of *Gobivenator*, *Philovenator*, and many dromaeosaurids (Russell and Dong, 1993; Norell and Makovicky, 2004; Xu et al., 2012; Tsuihiji et al., 2014).

EGGSHELL ASSOCIATED WITH IGM 100/1323

Six small eggshell fragments are scattered in close proximity to the skeleton. One is just ventral to the right mandible (fig. 2), another is lateral to the left mandible near the jaw joint (fig. 3), and another is located between the legs, underneath the left femur and a displaced vertebra (fig. 9). Two others are on a small block of matrix prepared away from the specimen. A 7.6 × 8.6 mm fragment located about 21 mm away from the right ilium (fig. 16A) was sampled for radial thin sectioning and microstructural examination with a petrographic microscope (Leitz Laborlux 11 POL S; Leitz Inc., Wetzlar, Germany) and a scanning electron microscope (SEM) (Zeiss EVO 60 Variable Pressure, Zeiss Inc., Jena, Germany). Measurements of the photomicrographs and SEM images were made using image-analysis software (ImageJ, NIH, Bethesda, Maryland).

The external surface of the eggshell is smooth. The sampled fragment measures 0.40 mm thick on average. The microstructure has been diagenetically altered; however, some of the original features are still visible. As in prismatoolithid and avian eggshells, there is an inner mammillary layer (ML) and an outer prismatic layer (PL) separated by a gradational boundary (fig. 16B,C). The mammillary layer is 0.12 mm thick on average and consists of cones comprised of blade-shaped calcite crystals that radiate outward from the innermost surface of the eggshell. Nucleation sites are not clearly preserved, as the inner surface is slightly eroded. The prismatic layer averages 0.28 mm in thickness and contains narrow, columnar prisms. The boundaries of the prisms are only faintly visible due to alteration. The PL:ML thickness ratio is approximately 2.3:1. Squamatic structure, a feature common to many theropod and avian eggs (e.g., Mikhailov, 1997a; Zelenitsky et al., 2002), is not obviously present, either due to biological absence or recrystallization. Small (1–3 μm diameter) vesicles are present throughout the PL. These may be the same as vesicles associated with squamatic structure in other theropod and avian eggs (Mikhailov, 1997a; Varricchio et al., 2002; Zelenitsky et al., 2002). Their slight enlargement relative to vesicles in most extant avian eggshell (Mikhailov, 1997a) could be explained by dissolution during recrystallization. Though the outermost portion of the prismatic layer exhibits a continuous dark-colored band (fig. 16C), this does not correspond to any obvious change in eggshell structure as seen under SEM (fig. 16B). Thus, due to recrystallization, it cannot be determined whether an external zone, such as that of *Troodon formosus* and most bird eggshells (Mikhailov, 1997a; Jackson et al., 2010; Varricchio and Barta, 2015), is present. The eggshell is covered with a layer of diagenetic calcite up to 0.06 mm thick. No pores are visible in the sampled fragment.

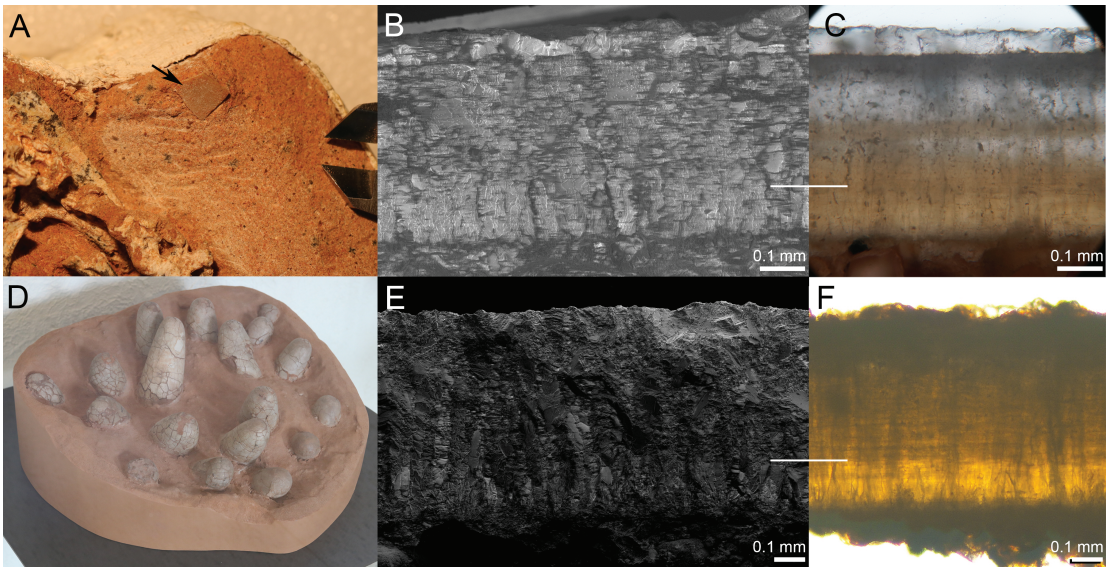

FIGURE 16. **A.** IGM 100/1323, arrow indicates sampled eggshell fragment. Caliper edges are 5 mm apart. **B.** IGM 100/1323, eggshell under SEM. Line indicates boundary between mammillary (below line) and prismatic (above line) layers. **C.** IGM 100/1323, eggshell thin section under plane polarized light. Line indicates boundary between mammillary (below line) and prismatic (above line) layers. **D.** AMNH FARB 6631, clutch of 18 eggs, prepared with their bottom surfaces upwards. **E.** AMNH FARB 6631, eggshell under SEM. Line indicates boundary between mammillary (below line) and prismatic (above line) layers. **F.** AMNH FARB 6631, eggshell thin section under plane polarized light. Line indicates boundary between mammillary (below line) and prismatic (above line) layers.

IGM 100/1323 has thicker eggshell than probable avian oospecies from Gobi Campanian formations, including *Gobioolithus minor*, *G. major*, and *Styloolithus sabathi* (Mikhailov, 1996a; Varricchio and Barta, 2015), suggesting that the eggshell is indeed from a nonavian dinosaur. IGM 100/1323 eggshell also has a greater PL:ML ratio than the Mongolian oospecies *Laevisoolithus sochavai* and *Subtiliolithus microtuberculatus*, which may also be small nonavian theropod or avian eggs (Mikhailov, 1991). IGM 100/1323 eggshell probably lacks the clearly defined squamatic structure and external zone of *Parvoolithus tortuosus* (Zelenitsky, 2004; also see Mikhailov, 1996b: fig. 1d). Among prismatoolithid eggs, IGM 100/1323 has thinner eggshell than that from the equator and upper pole of *Protoceratopsidovum fluxuosum* eggs, and lacks the surface ornamentation of that oospecies (Mikhailov, 1994). IGM 100/1323 has a greater PL:ML thickness ratio than *Protoceratopsidovum sincerum* (Varricchio and Barta, 2015). It most closely resembles *Protoceratopsidovum minimum* in total eggshell thickness (Mikhailov, 1994) and PL:ML thickness ratio (Varricchio and Barta, 2015). IGM 100/1323 eggshell and eggshell adhering to a perinatal troodontid skull (IGM 100/972) have similar thicknesses, but IGM 100/1323 has a higher PL:ML thickness ratio than that of IGM 100/972 (Grellet-Tinner, 2006).

We assign the eggshell associated with *Almas ukhaa* (IGM 100/1323) to the Prismatoolithidae (Hirsch, 1994; Zelenitsky and Hills, 1996) based on the aforementioned smooth surface, eggshell thickness, and microstructural characteristics. Given diagenetic obfuscation of other features and the fragmentary preservation, we can assign the eggshell only to Prismatoolithidae

indet., but we note that its preserved attributes are most similar to *Protoceratopsidovum minimum*. The only unequivocal taxonomic assignments for Cretaceous prismatoolithid eggs come from associations with troodontid skeletal remains, including *Troodon formosus* embryos in *Prismatoolithus levis* eggs (Horner and Weishampel, 1996; Varricchio et al., 2002, Jackson et al., 2010), an adult *Troodon formosus* contacting a *Prismatoolithus levis* egg clutch (Varricchio et al., 1997), and prismatoolithid eggshell associated with troodontid perinates (Norell et al., 1994; Grellet-Tinner, 2005; Grellet-Tinner, 2006; Bever and Norell, 2009). An alternative assignment of *Protoceratopsidovum* eggs to neoceratopsians (Mikhailov, 1994, 1997b, 2000, 2014) is based on the relative abundance of neoceratopsian remains at the same localities at which the eggs are found, although close associations of perinate or adult neoceratopsians with eggs are currently unknown (Varricchio et al., 2015). Given the strong correlation of prismatoolithid eggs with troodontids, it is plausible that the eggshell associated with *Almas ukhaa* was laid by that taxon. However, accidental association or predation by *Almas ukhaa* upon the eggs of a different taxon cannot be ruled out at this time.

The eggshell microstructure of AMNH FARB 6631 (Granger, 1936; Brown and Schlaikjer, 1940), a clutch of 18 prismatoolithid eggs from the Djadokhta Formation at Bayn Dzak (fig. 16D), has to our knowledge never before been published. As discussed by Thulborn (1992), the subvertical arrangement of eggs in this clutch is very similar to eggs that were later found to be those of *Troodon formosus* (Horner and Weishampel, 1996) from the Campanian Egg Mountain locality, Montana. Thus, as a probable troodontid clutch from the Djadokhta Formation, AMNH FARB 6631 provides additional data for comparison with IGM 100/1323. We thin-sectioned and examined with SEM an isolated, unornamented eggshell fragment (fig. 16E, F) collected from the same locality (Chouji Cliffs at Bayn Dzak) in the same year (1925) and cataloged under the same specimen (6631 and 6630) and field (526) numbers as the egg clutch currently displayed in the AMNH Hall of Ornithischian Dinosaurs. Some fragments in the same box are labeled "6630," but these likely also originate from the egg clutch, as plate 12 of Brown and Schlaikjer (1940) shows that this specimen number was formerly applied to at least one egg in the clutch now cataloged as AMNH FARB 6631. Despite the presence of two fragments of ornamented elongatoolithid eggshell in the same box as the sampled specimen, we can be reasonably confident that the more numerous smooth-surfaced eggshells are those that weathered away from or were prepared off the clutch on exhibition.

The eggshell of AMNH FARB 6631 is thicker than that of IGM 100/1323, averaging 0.65 mm thick and consisting of a 0.16 mm thick mammillary layer and the overlying 0.49 mm thick prismatic layer, within which the prismatic columns are clearly visible. Under SEM (fig. 16E), some prisms contain what resembles patchy squamatic structure, as in the eggs of *Troodon formosus* (*Prismatoolithus levis*) (Zelenitsky et al., 2002). Vesicles similar to those of IGM 100/1323 and *Prismatoolithus levis* (Varricchio et al., 2002; Zelenitsky et al., 2002) are present in the prismatic layer. The average PL:ML thickness ratio is 3.1:1, greater than that of IGM 100/1323, IGM 100/972 (Grellet-Tinner, 2006), *Prismatoolithus levis* (Jackson et al., 2010), *Protoceratopsidovum sincerum*, and *Protoceratopsidovum minimum* (Varricchio and Barta, 2015). The outer 0.12 mm of the prismatic layer shows a subtle structural change to "blockier" ultrastructure, with some

visible prism boundaries, compared to the columnar prisms below (fig. 16E). This zone appears darker in thin section (fig. 16F), and possibly represents an external zone as in *Prismatoolithus levis* and avian eggshell (Mikhailov, 1997a; Jackson et al., 2010). However, given the difficulties in interpreting the presence of an external zone in diagenetically altered eggs (Mikhailov, 2014; Varricchio and Barta, 2015), it remains unclear whether this outer zone is an original, biological feature. No pores are visible in the sampled fragment. The AMNH FARB 6631 eggs are too large to be those of *Almas ukhaa* and were probably laid by a larger-bodied troodontid. Similarities with *Troodon formosus* eggshell, including the patchy squamatic structure and possible external zone, further support this. Based on the above microstructural features, eggshell thickness, smooth eggshell surface, asymmetric egg shape, and subvertical arrangement of eggs in the clutch, we assign AMNH FARB 6631 to *Prismatoolithus* oosp. (Zhao and Li, 1993; Zelenitsky and Hills, 1996). Assigning AMNH FARB 6631 to a particular oospecies would require further review of all *Prismatoolithus* oospecies and is outside the scope of this study.

At least five different prismatoolithid egg varieties are known from Djadokhta-equivalent formations in Mongolia and China (Zhao and Li, 1993, Mikhailov, 1994; Grellet-Tinner, 2006), similar to the number of troodontid taxa known from skeletal remains from these formations. However, with a few notable exceptions (e.g., Erickson et al., 2007; Bever and Norell, 2009) associations of eggs or eggshell with Djadokhta troodontid skeletal remains are rare, hindering potential correlations of taxonomic and ootaxonomic diversity. Based on the smooth eggshell surface, eggshell thickness, and microstructural characteristics, it remains plausible that the eggshell associated with IGM 100/1323 is that of *Almas ukhaa*. Despite this, we cannot definitively assign the eggshell to this taxon because it is difficult to narrow down our multiple hypotheses about how the skeleton and eggshell came to be preserved together.

DISCUSSION

Comparisons with Other Troodontid Taxa from the Djadokhta Formation

Three other named troodontid taxa have been reported from the Djadokhta Formation of Mongolia. *Saurornithoides mongoliensis* was the first troodontid dinosaur reported from the Djadokhta Formation in 1924, based on a weathered skull with an articulated mandible and fragmentary postcranial bones (Osborn, 1924). *Byronosaurus jaffei* was reported in 2000, based on two adult specimens with partial cranial and fragmentary postcranial bones (Norell et al., 2000). *Gobivenator mongoliensis* was described in 2014, based on an almost complete cranium and most of the postcranium of an adult individual (Tsuihiji et al., 2014).

Unlike *Almas ukhaa*, adult specimens of *Saurornithoides*, *Byronosaurus*, and *Gobivenator* all share an elongate rostrum and a relatively larger body size (skull length ~20 cm). This is in agreement with the Early Cretaceous *Sinornithoides* and other later-diverging troodontids such as *Troodon* and *Zanabazar* (Currie and Dong, 2001; Makovicky et al., 2003; Norell et al., 2009). Though *Almas ukhaa* resembles more basal troodontids (e.g., *Sinovenator*, *Mei*, *Jinfengopteryx*, *Sinusonasus*) in having a relatively smaller size and a

short rostrum, these Djadokhta troodontids share other derived troodontid features. In the cranium, all four Djadokhta taxa feature a well-defined pneumatic lateral depression on the braincase, an external naris positioned entirely anterior to the antorbital fossa, a lateral groove on the ventral ramus of the maxilla, a broad lateral lamina of the ascending process of the maxilla, a reduced maxillary toothrow that does not reach the posterior end of the maxilla, and a laterally recessed squamosal. All these features are derived characters that are absent in more basal troodontids such as *Sinovenator*, *Mei*, *Sinusonasus*, *Jinfengopteryx*, *Sinornithoides*, and IGM 100/44. The ischium of *Almas ukhaa* is more than half the length of the pubis. This was regarded as a primitive feature of *Almas ukhaa* because basal maniraptorans tend to have longer ischia (Turner et al., 2012). But new observations from *Anchiornis*, *Talos*, *Gobivenator*, and *Almas ukhaa* indicate that a short ischium is primitive for paravians, and a longer ischium is secondarily acquired in later-diverging troodontids (Zanno et al., 2011; Tsuihiji et al., 2014; Pei et al., 2017). Therefore, the elongate ischium of *Almas ukhaa* is actually a synapomorphy of an anatomically more derived troodontid clade.

Almas ukhaa differs from *Saurornithoides*, *Byronosaurus*, and *Gobivenator* in many features, most of which are primitive troodontid features of the cranial skeleton, especially of the rostrum. Structures of the maxilla, including the antorbital fossa, maxillary fenestra, and antorbital fenestra, are proportionally shorter in *Almas ukhaa* than in other named Djadokhta troodontids. Unlike in *Saurornithoides*, *Byronosaurus*, and *Gobivenator*, but as in most Early Cretaceous troodontids, the ventral process of the lacrimal inclines anterodorsally in *Almas ukhaa*. *Almas ukhaa* also lacks a characteristic of most other troodontids, the lateral groove on the dentary.

Apart from the features mentioned above, *Almas ukhaa* also differs significantly from *Byronosaurus* in the number of maxillary teeth. Either 16 or 17 tooth positions are estimated on each maxilla of *Almas ukhaa*, which is congruent with the pattern seen in most other troodontids. However, in *Byronosaurus*, more than 30 maxillary teeth are estimated on each side (Makovicky et al., 2003). Both taxa have the typical troodontid pattern of tooth distribution, in which the anterior teeth are closely packed. *Byronosaurus* has much denser tooth positions than *Almas ukhaa*, as 10 teeth are located ventral to the maxillary fenestra in *Byronosaurus*, but only four are observed in the same part of *Almas ukhaa*. *Almas ukhaa* also differs from *Byronosaurus* in having an anteroposteriorly narrow interfenestral bar of the maxilla and an enlarged anterior tympanic recess excavated ventral to the anterior tympanic crista.

Almas ukhaa and *Gobivenator* share several similarities in the cranial and postcranial anatomy. Notably, both taxa have a prominent process on the anterior edge of the obturator process of the ischium. But unlike *Gobivenator*, this process is much more pronounced and becomes spikelike in *Almas ukhaa* (fig. 13). The ischia of *Almas ukhaa* remain unfused, whereas the ischia form a symphysis in *Gobivenator* and *Saurornithoides* (Norell et al., 2009; Tsuihiji et al., 2014). In addition, *Almas ukhaa* differs from *Gobivenator* in the presence of an anterolateral recess on the lacrimal, a straight ventral process of the lacrimal, a posteriorly curved pterygoid flange, and the absence of an anterior surangular foramen.

Despite the proportions of the rostral elements, *Almas ukhaa* is different from *Saurornithoides* in the absence of denticles on the maxillary teeth. Serrated teeth are observed in nearly all dromaeosaurids, and in many troodontids including *Sinovenator*, *Sinusonasus*, *Sinornithoides*, *Saurornithoides*, *Troodon*, *Zanabazar*, and *Linhevenator* (Xu et al., 2002; Xu and Wang, 2004; Norell et al., 2009; Xu et al., 2011a). Other troodontids such as *Mei*, *Gobivenator*, and *Byronosaurus* lack denticles on the maxillary teeth (Norell et al., 2000; Makovicky et a., 2003; Xu and Norell, 2004; Tsuihiji et al., 2014). *Saurornithoides* also differs from *Almas ukhaa* in having a shortened external naris and a U-shaped mandibular symphysis, both of which are synapomorphies of a later-diverging troodontid clade. The pterygoid flange of *Saurornithoides* is short and does not bear the posterior curvature that is present in *Almas ukhaa* (Norell et al., 2009).

A fragmentary troodontid specimen, IGM 100/1083, was described in 2004 from the Djadokhta Formation at Ukhaa Tolgod (Norell and Hwang, 2004). IGM 100/1083 has a broad lateral lamina of the ascending process of the maxilla, like most Late Cretaceous troodontids (except for the unnamed IGM 100/1126). It was provisionally referred to *Saurornithoides mongoliensis* based on stratigraphic occurrences, but it is too fragmentary and lacks definitive morphological features to be assigned to a named generic level taxon (Norell and Hwang, 2004).

Philovenator curriei was originally described as a juvenile *Saurornithoides mongoliensis* from the Wulansuhai Formation, Inner Mongolia, China, preserved with a partial hindlimb (Xu et al., 2012). *Linhevenator tani* was also reported from the Wulansuhai Formation, Inner Mongolia, China based on a partial skeleton (Xu et al., 2011a). *Almas* resembles both *Philovenator* and *Linhevenator* in having a laterally recessed squamosal (squamosal not preserved in *Philovenator*), a ridgelike longitudinal posterior trochanter on the posterior surface of the femur, the astragalus and the calcaneum cofused (not exposed in *Linhevenator*) and a much narrower metatarsal II than metatarsal IV. Unlike *Almas*, the distal tarsals are completely fused to metatarsals in *Philovenator*, and the hind-limb elements—the femur, the tibia, and the metatarsus—appear distinctly transversely compressed (Xu et al., 2012). *Linhevenator*, however, is more similar to *Saurornithoides* in having serrated premaxillary teeth and a bladelike distal portion of the ischium, in contrast to the unserrated teeth and the lobelike distal ischium in *Almas ukhaa*.

Many features shared by these named Djadokhta troodontids and *Almas ukhaa* are also present in other Late Cretaceous troodontids (e.g., *Troodon*, *Zanabazar*, *Xixiasaurus*, *Talos*, and *Tochisaurus*), such as a well-defined pneumatic lateral depression on the braincase, a well-developed subotic recess, an external naris positioned entirely anterior to the antorbital fossa, a broad lateral lamina of the ascending process of the maxilla, the promaxillary fenestra not exposed in lateral view, reduced length of the maxillary toothrow, a lacrimal with a longer anterior process than the posterior process and a much narrower metatarsal II than metatarsal IV. These features are likely the synapomorphies that unite these Late Cretaceous troodontids.

Comparisons with Troodontids from Northeastern China

Almas ukhaa has a body plan similar to basal paravians and troodontids from the Jehol Biota of northeastern China (e.g., *Sinovenator*, *Jianianhualong*, *Sinusonasus*, *Mei*, and *Jinfengopteryx*) in having a small body size, a relatively short snout, and a large orbit (Xu et al., 2002; Xu and Norell, 2004; Xu and Wang, 2004; Ji and Ji, 2007; Xu et al., 2017). However, it lacks many primitive features that are present in the Jehol troodontids, such as an external naris that posteriorly overlaps the anterior margin of the antorbital fossa, a deep anterior ramus of the maxilla, a reduced lateral lamina of the maxilla, the absence of a subotic recess, and metatarsal II almost as transversely wide as metatarsal IV. These characters are plesiomorphic for all paravians, but are not reported in Late Cretaceous troodontids such as *Almas ukhaa*, *Byronosaurus*, *Gobivenator*, *Saurornithoides*, *Zanabazar*, and *Troodon* (Makovicky et al., 2003; Norell et al., 2009; Lü et al., 2010; Tsuihiji et al., 2014). A subarctometatarsalian pes is reported in the basal troodontid *Sinovenator* as an intermediate state between the normal pes of other paravians and the typical arctometatarsalian pes of derived troodontids (Xu et al., 2002). Although *Sinusonasus* is also reported with an arctometatarsalian condition (Xu and Wang, 2004), it resembles *Sinovenator* in having a metatarsal III with its proximal shaft only slightly constricted compared with its distal shaft in anterior view. In contrast, in *Almas ukhaa*, along with other Late Cretaceous troodontids, the proximal one-third of metatarsal III is either not exposed anteriorly or strongly constricted compared with the distal one-third of the shaft.

Sinornithoides, another Early Cretaceous troodontid from China, has a larger body size and proportionally longer snout than *Almas ukhaa* and the Jehol troodontids (Russell and Dong, 1993). Unlike *Sinornithoides*, *Almas ukhaa* has a broad lateral lamina of the ascending process of the maxilla, an elongate ischium, and metatarsal IV significantly more robust than metatarsal II. Notably, these characters are also present in derived troodontids of the Late Cretaceous, but are absent in the more basal Jehol troodontids, which may indicate that *Almas ukhaa* is a more derived troodontid than the larger-bodied *Sinornithoides*. Besides, *Almas ukhaa* is also different from *Sinornithoides* in having teeth without serrations and a distinct anterior spike on the obturator process of the ischium.

The Jehol troodontids (*Sinovenator*, *Jianianhualong*, *Sinusonasus*, *Mei*, and *Jinfengopteryx)* and *Almas ukhaa* all share a short and relatively deep rostrum that is a typical pedomorphosis of basal paravian skulls (Bhullar et al., 2012). Other derived Late Cretaceous troodontids, such as *Byronosaurus*, *Gobivenator*, *Linhevenator*, *Saurornithoides*, *Zanabazar*, and *Troodon*, are characterized by a proportionally longer rostrum where the maxilla and the nasal are significantly elongate (Norell et al., 2000; Norell et al., 2009; Xu et al., 2011a; Tsuihiji et al., 2014). A series of structural transformations is associated with the elongation of the rostrum, such as the elongation of the maxillary fenestra, antorbital fenestra, and nasal, and the anterior shift of the ventral process of the lacrimal. A body-size increase is also observed in derived Late Cretaceous troodontids, along with the elongation of rostrum, like the pattern observed in dromaeosaurids (Turner et al., 2007b). Even though *Almas ukhaa* has a primitive paravian configuration of a shortened rostrum like Jehol troodontids, it resembles derived Late Creta-

ceous troodontids in nonproportional rostral morphologies. These morphologies include the external naris located well anterior to the anterior margin of the antorbital fossa, a broad lateral lamina of the ascending process of the maxilla, the promaxillary fenestra not exposed in lateral view and reduced length of the maxillary toothrow. *Almas ukhaa* resembles only the primitive Jehol troodontids in general cranial proportions, but its nonproportional rostral anatomies are similar to the more closely related Late Cretaceous troodontids, which indicates that pedomorphism in *Almas* was achieved by retaining only the general proportion of a juvenile skull without the primitive nonproportional rostral morphologies.

Comparisons with the Ukhaa Perinates IGM 100/972 and IGM 100/974

Two perinate troodontid specimens (IGM 100/972 and IGM 100/974) were described from the Djadokhta Formation of Ukhaa Tolgod (Bever and Norell, 2009). These specimens are represented by partial snouts, a partial braincase (including the dermal roof), and an associated nest of hatched eggs. The Bever and Norell (2009) study regarded the perinates as most closely related to *Byronosaurus jaffei* and placed them into an expanded *Byronosaurus* without equating them to *B. jaffei* or erecting a new species-level name. The subsequent description of *Gobivenator* (Tsuihiji et al., 2014) and now *Almas ukhaa* erodes support for a privileged relationship between the Ukhaa perinates and *Byronosaurus* and suggests the perinates could possibly be juveniles of a range of Late Cretaceous troodontids, but more likely are more closely related to *Almas ukhaa* based on a potential derived morphology.

IGM 100/972 and IGM 100/974 share many features with other Djadokhta troodontids such as *Almas ukhaa*, *Byronosaurus*, *Gobivenator*, and *Saurornithoides*. Both of the Ukhaa perinate specimens have a broad lateral lamina of the ascending process of the maxilla, a maxillary toothrow that does not reach the posterior end of the maxilla, and an external naris that is entirely anterior to the antorbital fossa. All these are characters shared by a group of derived troodontids that includes *Almas ukhaa*, *Byronosaurus*, *Gobivenator*, and *Saurornithoides*.

Evidence for the referral of IGM 100/972 and IGM 100/974 as perinate *Byronosaurus* was based on the presence of a lateral groove on the ventral ramus of the maxilla (Bever and Norell, 2009). However, the presence of this feature in *Gobivenator*, *Almas ukhaa*, and on the left maxilla of *Saurornithoides* suggests that it diagnoses a more inclusive clade, but one that is still deeply nested within the troodontid radiation. IGM 100/972 and IGM 100/974 are estimated to have 13–15 maxillary teeth on each side, similar to that of *Gobivenator* (19), *Almas ukhaa* (17), and *Saurornithoides* (19), but significantly fewer than in *Byronosaurus jaffei* (more than 30). The increase in the number of maxillary teeth is regarded as an ontogenetic trend in several theropod dinosaurs (Rauhut and Fechner, 2005), but the difference between *Byronosaurus jaffei* and the Ukhaa perinates is perhaps beyond what might be expected for a single postnatal transformation, even though a postnatal transformation from 13–15 teeth to more than 30 teeth was not necessarily assumed while the perinates were placed as *Byronosaurus* (Bever and Norell, 2009).

The prootic of the Ukhaa perinate IGM 100/974 also differentiates it from adult *Byronosaurus jaffei*. IGM 100/974 has a prootic with an anterior tympanic recess excavated ventral to the anterior tympanic crista, as in *Almas ukhaa*, *Saurornithoides*, and *Troodon* (Currie and Zhao, 1993; Norell et al., 2009), but different from *Byronosaurus*, in which the anterior tympanic recess is groovelike instead of excavated ventral to the anterior tympanic crista (Makovicky et al., 2003). In addition, as in *Almas ukhaa*, the dorsal tympanic recess of IGM 100/974 lacks a foramen that is present in *Byronosaurus*.

As in *Almas ukhaa*, *Byronosaurus*, and *Saurornithoides*, the Ukhaa perinates could be differentiated from *Gobivenator* in having an anterolateral recess on the lacrimal. The interfenestral bar of the Ukhaa perinates is anteroposteriorly narrow as in *Almas ukhaa* and *Saurornithoides* (Norell et al., 2009), but differs from the widened condition in *Gobivenator* and *Byronosaurus* (Makovicky et al., 2003; Tsuihiji et al., 2014). The teeth of IGM 100/972 and IGM 100/974 lack serrations on either anterior or posterior carinae, as in *Almas ukhaa*, *Byronosaurus*, and *Gobivenator*, but differing from *Saurornithoides*. The anterior portion of the dentary of the Ukhaa perinates lacks the lateral groove that is typical of troodontids, a condition also seen in *Almas ukhaa*, but different from that of *Byronosaurus*, *Gobivenator,* and *Saurornithoides*. This could be a potential derived feature that unites the Ukhaa perinates and *Almas*, but the polarity and thus taxonomic significance of this feature awaits a more comprehensive phylogenetic analysis of troodontids.

As inferred from the morphology of the maxilla, the dentition, and the prootic, the Ukhaa perinates can be confidently put into a derived Late Cretaceous troodontid clade that also includes *Almas ukhaa*, *Byronosaurus*, *Gobivenator*, and *Saurornithoides*, but a unique close relationship between the Ukhaa perinates and *Byronosaurus* is no longer supported. Among these troodontid taxa, the Ukhaa perinates possibly resemble *Almas ukhaa* more closely in having a smooth lateral surface at the anterior part of the dentary. However, the taxonomic affiliation of the Ukhaa perinates still cannot be determined definitively because no solid derived features are found to ally them with any one reported troodontid species. The Ukhaa perinates IGM 100/972 and IGM 100/974 have a higher chance of being closely related to *Almas ukhaa*, but they are probably not the same taxon also because both specimens were found in a nest of eggs with sizes that are too large to be those of *Almas ukhaa*.

Common rostral features of *Almas ukhaa*, *Byronosaurus*, *Gobivenator*, and *Saurornithoides* are employed as an ontogenetically more developed comparison of the Ukhaa perinates, to investigate the trend of postnatal transformation of this Late Cretaceous troodontid clade. As perinatal individuals, IGM 100/972 and IGM 100/974 have allometric variations relative to *Almas ukhaa*, *Byronosaurus*, *Gobivenator*, and *Saurornithoides* in general scaling of the skull. The orbit is proportionally larger in the Ukhaa perinates than in those taxa. The rostral elements, such as the maxilla and the nasal of the Ukhaa perinates, are proportionally shorter than in *Almas ukhaa*, *Byronosaurus*, *Gobivenator*, and *Saurornithoides*. Therefore, postnatal elongation of the rostrum occurs in troodontids as in other archosaurs (Coombs, 1982; Carr, 1999; Rauhut and Fechner, 2005; Bhullar et al., 2012). These differences in scaling and a trend of rostral elongation were also proposed by Bever and Norell (2009) while comparing the Ukhaa perinates with *Byronosaurus jaffei* alone. Despite the elongation of the rostrum, the

nonproportional morphologies, and proportions within the antorbital fossa remain relatively constant in the Ukhaa perinates, *Almas ukhaa* and even more anatomically derived troodontids with elongate snouts, such as *Byronosaurus*, *Gobivenator*, and *Saurornithoides* (Makovicky et al., 2003; Norell et al., 2009; Tsuihiji et al., 2014)

The prootic of IGM 100/974 closely resembles that of *Almas ukhaa* and *Saurornithoides*, and the postnatal transformation of the prootic is not as significant as determined in the Bever and Norell study (2009), where a comparison was made between IGM 100/974 and *Byronosaurus jaffei*. Compared to IGM 100/974, *Almas ukhaa* and *Saurornithoides* exhibit an enlarged anterior tympanic recess and a more pronounced anterior tympanic crista, but other structures of the prootic are similar in these specimens. This may imply that the postnatal changes of the braincase are mainly proportional rather than structural in this derived troodontid clade.

SUMMARY

Almas ukhaa represents a new troodontid taxon from the Late Cretaceous Djadokhta Formation at Ukhaa Tolgod. This new taxon is diagnosed as distinct from other troodontids by: presence of a posteriorly curved pterygoid flange, absence of a lateral groove on the anterior part of the dentary, presence of a distinct ventral spikelike process on the ischium, and elongate proximal chevrons.

Although *Almas ukhaa* has a small body size and a short snout as in basal paravians, it bears many derived troodontid features, such as a well-defined pneumatic lateral depression on the braincase, an external naris positioned entirely anterior to the antorbital fossa, a broad lateral lamina of the ascending process of the maxilla, the promaxillary fenestra not exposed in lateral view, reduced length of the maxillary toothrow, and a much narrower metatarsal II than metatarsal IV. Based on these derived features, *Almas* is likely closely related to other Late Cretaceous troodontids, and is more derived than the Early Cretaceous troodontids reported from China.

The eggshell associated with IGM 100/1323 can be assigned to Prismatoolithidae indet. based on the smooth surface, eggshell thickness, and microstructural characteristics. Although it cannot be definitively assigned to *Almas ukhaa*, it remains plausible that the eggshell is that of this taxon given the strong correlation of prismatoolithid eggs with troodontids.

The presence of a maxillary groove in *Almas ukhaa* and *Gobivenator* erodes support for a unique relationship between *Byronosaurus* and the Ukhaa perinates (IGM 100/972 and IGM 100/974). Instead, the Ukhaa perinates could be affiliated with a range of Late Cretaceous troodontids and preliminary evidence suggests that they are more closely related to *Almas ukhaa*.

ACKNOWLEDGMENTS

We thank the Mongolian Academy of Sciences, and the members of the 1993 expedition. This specimen was prepared by Amy Davidson. Mick Ellison provided the figures. We thank

John Flynn, Meng Jin, Peter Makovicky, and Alan Turner for reading the manuscript and providing useful advice. Morgan Hill provided assistance with scanning electron microscopy, and Saebyul Choe, Beth Goldoff, and D. Ebel provided access to thin-sectioning equipment and facilities. We also thank both reviewers for their insightful comments on this manuscript. This work was supported by the Division of Paleontology, American Museum of Natural History, the Newt and Callista Gingrich Fund and the Macaulay family. Support to Pei Rui was also given by Columbia University and the University of Hong Kong. Daniel Barta is supported by a Richard Gilder Graduate School Fellowship. Xu Xing was supported by the National Science Foundation of China (41688103). Michael Pittman was supported by the University of Hong Kong Faculty of Science.

REFERENCES

Averianov, A.O., and H.D. Sues. 2007. A new troodontid (Dinosauria: Theropoda) from the Cenomanian of Uzbekistan, with a review of troodontid records from the territories of the former Soviet Union. Journal of Vertebrate Paleontology 27 (1): 87–98.

Balanoff, A.M., and M.A. Norell. 2012. Osteology of *Khaan mckennai* (Oviraptorosauria: Theropoda). Bulletin of the American Museum of Natural History 372: 1–77.

Barsbold, R. 1974. Saurornithoididae, a new family of small theropod dinosaurs from central Asia and North America. Palaeontologia Polonica 30: 5–22.

Barsbold, R. 1983. [Carnivorous dinosaurs from the Late Cretaceous of Mongolia]. Sovmestnaya Sovetsko-Mongol'skaya Paleontologicheskaya Ekspiditsiya Trudy 19: 1–119. [in Russian]

Barsbold, R., and H. Osmólska. 1999. The skull of *Velociraptor* (Theropoda) from the Late Cretaceous of Mongolia. Acta Palaeontologica Polonica 44 (2): 189–219.

Barsbold, R., H. Osmólska, and S.M. Kurzanov. 1987. On a new troodontid (Dinosauria. Theropoda) from the Early Cretaceous of Mongolia. Acta Palaeontologica Polonica 32 (1–2): 121–132.

Bever, G.S., and M.A. Norell. 2009. The perinate skull of *Byronosaurus* (Troodontidae) with observations on the cranial ontogeny of paravian theropods. American Museum Novitates 3657: 1–51.

Bhullar, B.-A.S., et al. 2012. Birds have paedomorphic dinosaur skulls. Nature 487: 223–226.

Brown, D.B., and D.E.M. Schlaikjer. 1940. The structure and relationships of *Protoceratops*. Transactions of the New York Academy of Sciences 2: 99–100.

Brusatte, S.L., T.D. Carr, G.M. Erickson, G.S. Bever, and M.A. Norell. 2009. A long-snouted multihorned tyrannosaurid from the Late Cretaceous of Mongolia. Proceedings of the National Academy of Sciences of the United States of America 106: 17261–17266.

Brusatte, S.L., et al. 2013. The osteology of *Balaur bondoc*, an island-dwelling dromaeosaurid (Dinosauria: Theropoda) from the Late Cretaceous of Romania. Bulletin of the American Museum of Natural History 374: 1–100.

Brusatte, S.L., G.T. Lloyd, S.C. Wang, and M.A. Norell. 2014. Gradual assembly of avian body plan culminated in rapid rates of evolution across the dinosaur-bird transition. Current Biology 24: 2386–2392.

Burnham, D.A., et al. 2000. Remarkable new birdlike dinosaur (Theropoda: Maniraptora) from the Upper Cretaceous of Montana. University of Kansas Paleontological Contributions New Series 13: 1–14.

Carr, T.D. 1999. Craniofacial ontogeny in the Tyrannosauridae (Dinosauria, Coelurosauria). Journal of Vertebrate Paleontology 19: 497–520.

Chiappe, L.M., M.A. Norell and J.M. Clark. 1998. The skull of a relative of the stem-group bird *Mononykus*. Nature 392: 275–278.

Chiappe, L.M., M.A. Norell, and J.M. Clark. 2001. A new skull of *Gobipteryx minuta* (Aves: Enantiornithes) from the Cretaceous of the Gobi Desert. American Museum Novitates 3346: 1–15.

Claessens, L.A.P. 2004. Dinosaur gastralia: origin, morphology and function. Journal of Vertebrate Paleontology 24: 89–106.

Clark, J.M., M.A. Norell, and R. Barsbold. 2001. Two new oviraptorids (Theropoda: Oviraptorosauria) Upper Cretaceous Djadoktha Formation, Ukhaa Tolgod, Mongolia. Journal of Vertebrate Paleontology 21 (2): 209–213.

Coombs, W.P., Jr. 1982. Juvenile specimens of the ornithischian dinosaurs *Psittacosaurus*. Palaeontology 25: 89–107.

Csiki, Z., M. Vremir, S.L. Brusatte, and M.A. Norell. 2010. An abberant island dwelling theropod fromt the Late Cretaceous of Romania. Proceedings of the National Academy of Sciences of the United States of America 107 (35): 15357–15361.

Currie, P.J. 1985. Cranial anatomy of *Stenonychosaurus inequalis* (Saurischia, Theropoda) and its bearings on the origin of birds. Canadian Journal of Earth Sciences 22: 1643–1658.

Currie, P.J. 1995. New information on the anatomy and relationships of *Dromaeosaurus albertensis* (Dinosauria: Theropoda). Journal of Vertebrate Paleontology 15: 576–591.

Currie, P.J., and Z. Dong. 2001. New information on Cretaceous troodontids (Dinosauria, Theropoda) from the People's Republic of China. Canadian Journal of Earth Sciences 38: 1753–1766.

Currie, P.J., and X. Zhao. 1993. A new troodontid (Dinosauria, Theropoda) braincase from the Dinosaur Park Formation (Campanian) of Alberta. Canadian Journal of Earth Sciences 30: 2231–2247.

Dashzeveg, D., et al. 2005. New stratigraphic subdivision, depositional environment, and age estimate for the Upper Cretaceous Djadokhta Formation, southern Ulan Nur Basin, Mongolia. American Museum Novitates 3498: 1–31.

Dingus, L., et al. 2008. The geology of Ukhaa Tolgod (Djadokhta Formation, Upper Cretaceous, Nemegt Basin, Mongolia). American Museum Novitates 3616: 1–40.

Erickson, G.M., K.C. Rogers, D.J. Varricchio, M.A. Norell, and X. Xu. 2007. Growth patterns in brooding dinosaurs reveals the timing of sexual maturity in non-avian dinosaurs and genesis of the avian condition. Biology Letters 3: 558–561.

Elżanowski, A. 2001. A new genus and species for the largest specimen of *Archaeopteryx*. Acta Paleontologica Polonica 46: 519–532.

Forster, C.A., S.D. Sampson, L.M. Chiappe, and D.W. Krause. 1998. The theropod ancestry of birds: new evidence from the Late Cretaceous of Madagascar. Science 279: 1915–1919.

Foth, C., H. Tischlinger, and O.W.M. Rauhut. 2014. New specimen of *Archaeopteryx* provides insights into the evolution of pennaceous feathers. Nature 511: 79–82.

Gao, K., and M.A. Norell. 2000. Taxonomic composition and systematics of Late Cretaceous lizard assemblages from Ukhaa Tolgod and adjacent localities, Mongolian Gobi Desert. Bulletin of the American Museum of Natural History 249: 1–118.

Gao, C., E.M. Morschhauser, D.J. Varricchio, J. Liu, and B. Zhao. 2012. A second soundly sleeping dragon: new anatomical details of the Chinese troodontid *Mei long* with implications for phylogeny and taphonomy. PLoS ONE 7 (9): e45203.

Gauthier, J.A. 1986. Saurischian monophyly and the origin of birds. *In* K. Padian (editor), The origin of birds and evolution of flight: 1–55. San Francisco: California Academy of Sciences Memoir.

Granger, W. 1936. The story of the dinosaur eggs. Natural History 38 (6): 21–25.

Grellet-Tinner, G. 2005. A phylogenetic analysis of oological characters: a case study of saurischian dinosaur relationships and avian evolution. Ph.D. dissertation, Department of Earth Sciences, University of Southern California.

Grellet-Tinner, G. 2006. Phylogenetic interpretation of eggs and eggshells: implications for phylogeny of Palaeognathae. Alcheringa 30: 141–182.

Hirsch, K.F. 1994. Upper Jurassic eggshells from the western interior of North America. *In* K. Carpenter, K.F. Hirsch, and J.R. Horner (editors), Dinosaur eggs and babies: 137–150. Cambridge: Cambridge University Press.

Horner, J.R., and D.B. Weishampel. 1996. Correction: a comparative embryological study of two ornithischian dinosaurs. Nature 383: 103.

Hu, D., L. Hou, L. Zhang, and X. Xu. 2009. A pre-*Archaeopteryx* troodontid theropod from China with long feathers on the metatarsal. Nature 461: 640–643.

Hwang, S.H., M.A. Norell, Q. Ji, and K. Gao. 2002. New specimens of *Microraptor zhaoianus* (Theropoda, Dromaeosauridae) from northeastern China. American Museum Novitates 3381: 1–44.

Jackson, F.D., J.R. Horner, and D.J. Varricchio. 2010. A study of a *Troodon* egg containing embryonic remains using epifluorescence microscopy and other techniques. Cretaceous Research 31: 255–262.

Jerzykiewicz, T., and D.A. Russell. 1991. Late Mesozoic stratigraphy and vertebrates of the Gobi basin. Cretaceous Research 12: 345–377.

Ji, Q., et al. 2005. First avialian bird from China (*Jinfengopteryx elegans* gen et. sp. nov.). Geological Bulletin of China 24: 197–210.

Ji S., and Q. Ji. 2007. *Jinfengopteryx* compared to *Archaeopteryx*, with comments on the mosaic evolution of long-tailed avialan birds. Acta Geologica Sinica (English edition) 81 (3): 337–343.

Lü, J., et al. 2010. A new troodontid theropod from the Late Cretaceous of central China, and the radiation of Asian troodontids. Acta Palaeontologica Polonica 55: 381–388.

Kurzanov, S.M., and H. Osmólska. 1991. *Tochisaurus nemegtensis* gen. et sp. n., a new troodontid (Dinosauria, Theropoda) from Mongolia. Acta Palaeontologia Polonica 36: 69–76.

Makovicky, P.J. 2008. Telling time from fossils: a phylogeny-based approach to chronological ordering of paleobiotas ordering of paleobiotas. Cladistics 24 (3): 350–371.

Makovicky, P.J., and M.A. Norell. 2004. Troodontidae. *In* D.B. Weishampel, P. Dodson, and H. Osmólska (editors), The Dinosauria: 184–195. Berkeley: University of California Press.

Makovicky, P.J., M.A. Norell, J.M. Clark, and T.E. Rowe. 2003. Osteology and relationships of *Byronosaurus jaffei* (Theropoda: Troodontidae). American Museum Novitates 3402: 1–32.

Makovicky, P.J., S. Apesteguıa, and F.L. Agnolın. 2005. The earliest dromaeosaurid theropod from South America. Nature 437: 1007–1011.

Maleev, E.A. 1954. New turtle-like reptile in Mongolia. Priroda 1954 (3): 106–108.

Mayr, G., B. Pohl, and D.S. Peters. 2005. A well-preserved *Archaeopteryx* specimen with theropod features. Science 310: 1483–1486.

Mayr, G., B. Pohl, S. Hartman, and D.S. Peters. 2007. The tenth skeletal specimen of *Archaeopteryx*. Zoological Journal of the Linnean Society 149: 97–116.

Mikhailov, K.E. 1991. Classification of fossil eggshells of amniotic vertebrates. Acta Palaeontologica Polonica 36: 193–238.

Mikhailov, K.E. 1994. Theropod and protoceratopsian dinosaur eggs from the Cretaceous of Mongolia and Kazakhstan. Paleontological Journal 28: 101–120.

Mikhailov, K.E. 1996a. Bird eggs in the Upper Cretaceous of Mongolia. Paleontological Journal 30: 114–116.

Mikhailov, K.E. 1996b. New genera fossil eggs from the Upper Cretaceous of Mongolia. Paleontological Journal 30: 122–124.

Mikhailov, K.E. 1997a. Avian eggshells: an atlas of scanning electron micrographs. British Ornithologists' Club Occasional Publication 3: 1–88.

Mikhailov, K.E. 1997b. Fossil and recent eggshell in amniotic vertebrates: fine structure, comparative morphology and classification. Special Papers in Palaeontology 56: 1–80.

Mikhailov, K.E. 2000. Eggs and eggshells of dinosaurs and birds from the Cretaceous of Mongolia. *In* M. Benton, M. Shishkin, D. Unwin, and E. Kurochnkin (editors), The age of dinosaurs in Russia and Mongolia: 560–572. Cambridge: Cambridge University Press.

Mikhailov, K.E. 2014. Eggshell structure, parataxonomy and phylogenetic analysis: some notes on articles published from 2002 to 2011. Historical Biology 26: 144–154.

Norell, M.A., and J. Clarke. 2001. A new fossil near the base of Aves. Nature 409: 181–184.

Norell, M.A., and S.H. Hwang. 2004. A troodontid dinosaur from Ukhaa Tolgod (Late Cretaceous Mongolia). American Museum Novitates 3446: 1–9.

Norell, M.A., and P.J. Makovicky. 1997. Important features of the dromaeosaur skeleton: information from a new specimen. American Museum Novitates 3215: 1–28.

Norell, M.A., and P.J. Makovicky. 2004. Dromaeosauridae. *In* D.B. Weishampel, P. Dodson, and H. Osmólska (editors), The Dinosauria: 196–209. Berkeley: University of California Press.

Norell, M.A., et al. 1994. A theropod dinosaur embryo and the affinities of the Flaming Cliffs dinosaur eggs. Science 266: 779–782.

Norell, M.A., J.M. Clark, L.M. Chiappe, and D. Dashzeveg. 1995. A nesting dinosaur. Nature 378: 774–776.

Norell, M.A., P.J. Makovicky, and J.M. Clark. 2000. A new troodontid from Ukhaa Tolgod, Late Cretaceous, Mongolia. Journal of Vertebrate Paleontology 20 (1): 7–11.

Norell, M.A., P.J. Makovicky, and J.M. Clark. 2004. The braincase of *Velociraptor*. *In* P.J. Currie, E.B. Koppelhus, M.A. Shugar, and J.L. Wright (editors), Feathered dinosaurs: 133–143. Bloomington: Indiana University Press.

Norell, M.A., et al. 2006. A new dromaeosaurid theropod from Ukhaa Tolgod (Ömnögov, Mongolia). American Museum Novitates 3545: 1–51.

Norell, M.A., et al. 2009. A review of the Mongolian Cretaceous dinosaur *Saurornithoides* (Troodontidae: Theropoda). American Museum Novitates 3654: 1–63.

Novas, F.E., and Puerta, P.F. 1997. New evidence concerning avian origins from the Late Cretaceous of Patagonia. Nature 387: 390–2.

Osborn, H.F. 1924. Three new Theropoda, Protoceratops zone, central Mongolia. American Museum Novitates 144: 1–12.

Osmólska H., E. Roniewicz, and R. Barsbold. 1972. A new dinosaur, *Gallimimus bullatus* n. gen., n. sp. (Ornithomimidae) from the Upper Cretaceous of Mongolia. Palaeontologia Polonica 27: 103–143.

Ostrom, J.H. 1976. *Archaeopteryx* and the origin of birds. Biological Journal of the Linnean Society 8: 91–182.

Pei, R., Q. Li, Q. Meng, K.-Q. Gao, and M.A. Norell. 2014. A new specimen of *Microraptor* (Theropoda: Dromaeosauridae) from the Lower Cretaceous of western Liaoning, China. American Museum Novitates 3821: 1–28.

Pei, R., Q. Li, Q. Meng, M.A. Norell, and K.-Q. Gao. 2017. New specimens of *Anchiornis huxleyi* (Theropoda: Paraves) from the Late Jurassic of northeastern China. Bulletin of the American Museum of Natural History 411: 1–66.

Rauhut, O.W.M., and R. Fechner. 2005. Early development of the facial region in a non-avian theropod dinosaur. Proceedings of the Royal Society of London B 272: 1179–1183.

Rincen, P.R. 1964. Almas still exists in Mongolia. Genus 20 (4): 186–192.

Russell, D.A., and Z.-M. Dong. 1993. A nearly complete skeleton of a new troodontid dinosaur from the Early Cretaceous of the Ordos Basin, Inner Mongolia, People's Republic of China. Canadian Journal of Earth Sciences 30: 2163–2173.

Schmitz, L., and R. Motani. 2011. Nocturnality in dinosaurs inferred from scleral ring and orbit morphology. Science 332: 705–8.

Senter, P., J.I. Kirkland, J. Bird, and J.A. Bartlett. 2010. A new troodontid theropod dinosaur from the Lower Cretaceous of Utah. PLoS ONE 5 (12): e14329.

Thulborn, R.A. 1992. Nest of the dinosaur *Protoceratops*. Lethaia 25: 145–149.

Tsuihiji, T., et al. 2014. An exquisitely preserved troodontid theropod with new information on the palatal structure from the Upper Cretaceous of Mongolia. Naturwissenschaften 101 (2): 131–142. [doi: 10.1007/s00114-014-1143-9]

Turner, A.H., S.H. Hwang, and M.A. Norell. 2007a. A small derived theropod from Öösh, Early Cretaceous, Baykhangor Mongolia. American Museum Novitates 3557: 1–27.

Turner, A.H., D. Pol., J.A. Clarke, G. Erickson and M.A. Norell. 2007b. A basal dromaeosaurid and size evolution preceding avian flight. Science 317: 1378–1381.

Turner, A.H., D. Pol, and M.A. Norell. 2011. Anatomy of *Mahakala omnogovae* (Theropoda: Dromaeosauridae), Tögrögiin Shiree, Mongolia. American Museum Novitates 3722: 1–66.

Turner, A.H., P.J. Makovicky, and M.A. Norell. 2012. A review of dromaeosaurid systematics and paravian phylogeny. Bulletin of the American Museum of Natural History 371: 1–206.

Varricchio, D.J., and D.E. Barta. 2015. Revisiting Sabath's "larger avian eggs" from the Gobi Cretaceous. Acta Palaeontologica Polonica 60: 11–25.

Varricchio, D.J., A.M. Balanoff, and M.A. Norell. 2015. Reidentification of avian embryonic remains from the Cretaceous of Mongolia. PLoS ONE 10: e0128458.

Varricchio, D.J., J.R. Horner, and F.D. Jackson. 2002. Embryos and eggs for the Cretaceous theropod dinosaur *Troodon formosus.* Journal of Vertebrate Paleontology 22: 564–576.

Varricchio, D.J., F. Jackson, J.J. Borkowski, and J.R. Horner. 1997. Nest and egg clutches of the dinosaur *Troodon formosus* and the evolution of avian reproductive traits. Nature 385: 247–250.

Walker, A.D. 1985. The braincase of *Archaeopteryx*. *In* M.K. Hecht, J.H. Ostrom, H. Viohl, and P. Wellnhofer (editors), The beginnings of birds: 123–134. Willibaldsburg: Freunde des Jura-Museums Eichstatt.

Wellnhofer, P. 1974. Das funfte Skelettexemplar von *Archaeopteryx*. Palaeontographica Abteilung A Palaeozoologie-Stratigraphie 147: 169–216.

Wellnhofer, P. 2009. *Archaeopteryx:* the icon of evolution. Munich: Verlag Dr. Friedrich Pfeil. 1–207.

Wilson, M.C., and P.J. Currie. 1985. *Stenonychosaurus inequalis* (Saurischia: Theropoda) from the Judith River (Oldman Formation) of Alberta: new findings on metatarsal structure. Canadian Journal of Earth Sciences 22: 1813–1817.

Witmer, L.M. 1990. The craniofacial air sac system of Mesozoic birds (Aves). Zoological Journal of the Linnaean Society 100: 327–378.

Witmer, L.M. 1997. The evolution of the antorbital cavity of archosaurs: a study in soft-tissue reconstruction in the fossil record with an analysis of the function of pneumaticity. Society of Vertebrate Paleontological Memoir 3: 1–73.

Xu, X. 2002. Deinonychosaurian fossils from the Jehol Group of western Liaoning and the coelurosaurian evolution. Ph.D. dissertation, Chinese Academy of Sciences, Beijing, 325 pp.

Xu, X., and M.A. Norell. 2004. A new troodontid dinosaur from China with avian-like sleeping posture. Nature 431: 838–841.

Xu, X., and X. Wang. 2004. A new troodontid (Theropoda: Troodontidae) from the Lower Cretaceous Yixian Formation of western Liaoning, China. Acta Geologica Sinica 78 (1): 22–26.

Xu, X., X. Wang, and X. Wu. 1999. A dromaeosaur dinosaur with filamentous integument from the Yixian Formation of China. Nature 401: 262–266.

Xu, X., M.A. Norell, X. Wang, P.J. Makovicky, and X. Wu. 2002. A basal troodontid from the Early Cretaceous of China. Nature 415: 780–784.

Xu, X., et al. 2008. A new feathered maniraptoran dinosaur fossil that fills a morphological gap in avian origin. Chinese Science Bulletin 54: 430–435.

Xu, X, Q.-W.Tan, C. Sullivan, F.-L. Han, and D. Xiao. 2011a. A short-armed troodontid dinosaur from the Upper Cretaceous of Inner Mongolia and its implications for troodontid evolution. PLoS ONE 6: 1–12.

Xu, X., H. You, K. Du, and F. Han. 2011b. An *Archaeopteryx*-like theropod from China and the origin of Avialae. Nature 475: 465–479.

Xu, X., Q. Zhao, C. Sullivan, Q. Tan, M. Sander, and Q. Ma. 2012. The taxonomy of the troodontid IVPP V 10597 reconsidered. Vertebrata PalAsiatica 50 (2): 140–150.

Xu, X. et al. 2015. The taxonomic status of the Late Cretaceous dromaeosaurid *Linheraptor exquisitus* and its implications for dromaeosaurid systematics. Vertebrata PalAsiatica 53 (1): 29–62.

Xu, X. et al. 2017. Mosaic evolution in an asymmetrically feathered troodontid dinosaur with transitional features. Nature Communications. 8: 14972. [doi: 10.1038/ncomms14972]

Zanno, L.E., D. J. Varricchio, P.M. O'Connor, A.L. Titus, and M.J. Knell. 2011. A new troodontid theropod, *Talos sampsoni* gen. et sp. nov., from the Upper Cretaceous Western Interior Basin of North America. PLoS ONE 9 (6): e24487.

Zelenitsky, D.K. 2004. Description and phylogenetic implications of extant and fossil oologic remains. Ph.D. dissertation, Department of Geology and Geophysics, University of Calgary.

Zelenitsky, D.K., and L.V. Hills. 1996. An egg clutch of *Prismatoolithus levis* oosp. nov. from the Oldman Formation (Upper Cretaceous), Devil's Coulee, southern Alberta. Canadian Journal of Earth Sciences 33: 1127–1131.

Zelenitsky, D.K., S.P. Modesto, and P.J. Currie. 2002. Bird-like characteristics of troodontid theropod eggshell. *Cretaceous Research* 23: 297–305.

Zhao, Z., and R. Li. 1993. First record of Late Cretaceous hypsilophodontid eggs from Bayan Manduhu, Inner Mongolia. Vertebrata PalAsiatica 31: 77–84.

APPENDIX

Anatomical Abbreviations

aof	antorbital fenestra
ap	anterior process
asop	anterior spike of the obturator process
as	astragalus
atr	anterior tympanic recess
bo	basioccipital
bpp	basipterygoid process
ca 1-11	caudal vertebra 1–11
cal	calcaneum
ca.v	caudal vertebrae
cf	crescentic fossa
ch	chevron
cp	cultriform process
cr	cochlear recess
ddp	distal dorsal process
dtr	dorsal tympanic recess
e-o	exoccipital-opisthotic
eos	epiotic surface of the supraoccipital
es	egg shell
ff	facial fossa
gas	gastralia
gf	glenoid fossa
l.an	left angular
l.d	left dentary
l.ec	left ectopterygoid
l.f	left femur
l.fi	left fibula
l.fr	left frontal
l.is	left ischium
l.j	left jugal
l.l	left lacrimal
llap	lateral lamina of the ascending process
l.m	left maxilla
l.n	left nasal
l.p	left pubis
l.po	left postorbital
l.pr	left prearticular
l.prm	left premaxilla
l.pt	left pterygoid
l.q	left quadrate
l.qj	left quadratojugal
l.sa	left surangular

l.t	left tibia
mf	maxillary fenestra
mt II-V	metatarsal II–V
na	naris
nc	nuchal crest
otc	otosphenoidal crest
pd	pneumatic duct
ptf	pterygoid flange
pua	pubic apron
pub	pubic boot
r.d	right dentary
r.f	right femur
r.fi	right fibula
r.fr	right frontal
r.i	right ilium
r.is	right ischium
r.ls	right laterosphenoid
r.m	right maxilla
r.n	right nasal
r.m	right maxilla
r.p	right pubis
r.prm	right premaxilla
r.pt	right pterygoid
rr	anterior ramus
r.t	right tibia
sf	surangular foramen
sl	sclerotic ring
soc	supraorbital crest
sqc	cleft on the squamosal
sqr	lateral recess of the squamosal
s.v.	sacral vertebrae
vcf	vestibulocochlear fossa
vp	ventral process
V	opening for cranial nerve V
VII	opening for cranial nerve VII
X, XI, XII	cranial nerve openings X, XI, XII

All issues of *Novitates* and *Bulletin* are available on the web (http://digitallibrary.amnh.org/dspace). Order printed copies on the web from:
http://shop.amnh.org/a701/shop-by-category/books/scientific-publications.html

or via standard mail from:

American Museum of Natural History—Scientific Publications
Central Park West at 79th Street
New York, NY 10024

♾ This paper meets the requirements of ANSI/NISO Z39.48-1992 (permanence of paper).